Syntheses and structures of some complexes containing M3(μ-dppm)3 moieties (M = Cu, Ag) linking C4M'Lx groups [M'Lx = Re(CO)3(But 2-bpy), Ru(dppe)Cp⋆]

M.I. Bruce, B.G. Ellis, J.-F. Halet, Boris Le Guennic, B.K. Nicholson, H. Sahnoune, N. Scoleri, B.W. Skelton, A.N. Sobolev, C.J. Sumby, et al.

Syntheses and structures of some complexes containing $M_3(\mu\text{-dppm})_3$ moieties (M = Cu, Ag) linking $C_4\{M'L_x\}$ groups $[M'L_x = Re(CO)_3(Bu^t_2\text{-bpy})$, $Ru(dppe)Cp^*]$

Michael I. Bruce[a,*], Benjamin G. Ellis[a], Jean-François Halet[c], Boris Le Guennic[c], Brian K. Nicholson[d], Hiba Sahnoune[c], Nancy Scoleri[a], Brian W. Skelton[b,e], Alexandre N. Sobolev[b], Christopher J. Sumby[a], Allan H. White[b,†], Natasha N. Zaitseva[a]

[a] *Department of Chemistry, School of Physical Sciences, University of Adelaide, South Australia 5005*

[b] *School of Chemistry and Biochemistry, M313, The University of Western Australia, Crawley, Western Australia 6009*

[c] *Institut des Sciences Chimiques de Rennes, UMR 6226 CNRS - Université de Rennes 1, F-35042 Rennes cedex, France*

[d] *Department of Chemistry, University of Waikato, Hamilton, New Zealand*

[e] *Current address: Centre for Microscopy, Characterization and Analysis, M010, The University of Western Australia, Crawley, Western Australia 6009, Australia*

_____

ABSTRACT

Reactions between $[Ru(C{\equiv}CC{\equiv}CH)(dppe)Cp^*]$ and $[M_2(NCMe)_x(dppm)_2]^{2+}$ (M = Cu, x = 4; Ag, x = 2) have given complexes containing $M_3(\mu\text{-}dppm)_3$ clusters attached to one or two $-C{\equiv}CC{\equiv}C[Ru(dppe)Cp^*]$ groups. Single crystal X-ray studies are recorded for $[\{M_3(\mu\text{-}dppm)_3\}\{\mu_3\text{-}C{\equiv}CC{\equiv}C[Ru(dppe)Cp^*]\}](BF_4)_2{\cdot}nS$ (M = Cu, Ag) [isomorphous (orthorhombic) for S = (ill-defined) acetone]. A different (triclinic) polymorph has also been defined for M = Ag, nS = 5THF. Together with $[\{Cu_3(\mu\text{-}dppm)_3\}\{\mu_3\text{-}C{\equiv}CC{\equiv}C[Ru(dppe)Cp^*]\}_2]PF_6{\cdot}4Me_2CO$, the structures definitively confirm the complexes as clear examples of mono- or bis-diyndiyl-M_3 systems, devoid of close approaches to the vacant M_3 faces of the former by counterions in the case of their acetone solvates, except in the case of the BF_4 counterion in the $AgBF_4$ / thf solvate. Cyclic voltammetric studies suggest that there are only weak electronic interactions between the ruthenium centres in the bis(diynyl) complexes, consequent upon weak overlaps between the carbon chain and the $M_3(\mu\text{-}dppm)_3$ clusters, as confirmed by DFT calculations on model complexes $[\{M_3(\mu\text{-}dHpm)_3\}\{C{\equiv}CC{\equiv}C[Ru(dHpe)Cp]\}_n]^{3-n}$ [n = 1, 2; dHpm = $CH_2(PH_2)_2$, dHpe = $H_2P(CH_2)_2PH_2$]. The complexes $[Ag_3Cl_2(dppm)_3]PF_6$, $[M_3(\mu\text{-}dppm)_3(X)\{\mu_3\text{-}C{\equiv}CC{\equiv}C[Re(CO)_3(Bu^t_2\text{-}bpy)]\}]PF_6$ (M = Cu, X = $C{\equiv}CC{\equiv}C[Re(CO)_3(Bu^t_2\text{-}bpy)]$; M = Ag; X = Cl), $[Ag_6(\mu\text{-}dppm)_4\{C{\equiv}CC{\equiv}C[Re(CO)_3(Bu^t_2\text{-}bpy)]\}_4](PF_6)_2$ have also been prepared and structurally characterised. In the M_3 clusters, some asymmetry in the attachment of at least one of the μ_3 ligands is apparent, which results from interactions with solvate molecules.

_____

1. Introduction

Complexes containing metal centres linked by a conjugated carbon bridge have attracted great attention because of their potential applications in molecular electronics [1-6]. Among these complexes, many diyndiyl compounds [{L_nM}C≡CC≡C{ML_n}] (where ML_n is a redox-active metal-ligand fragment) have been prepared with Mo [7], W [8], Mn [9], Re [10,11], Fe [12], Ru [13,14], Ru_2 [15,16], Os [17] or Pt [18,19]. These complexes show medium to strong electronic interactions between the two redox-active metal termini through the conjugated C_4 chain, detailed calculations using density functional theoretical (DFT) methods having afforded some insight into the mechanism of electron transfer. Some recent reviews are available,[20,21] while an extensive consideration of the application of quantum chemical methods to the descriptions of a variety of mixed-valence systems is also available.[22]

An exciting development in this chemistry has been the synthesis of bis(diyndiyl) complexes of the general formula [{L_nM}C≡CC≡C{$M''L''_p$}C≡CC≡C{$M'L'_m$}], in which a central metal-ligand fragment provides a link between two metalla-diyndiyl groups which may be the same or different. The evaluation of any electronic communication through the central organometallic moiety is of particular interest here because of the possibility of the central fragment acting as an insulator, a conductor, or an amplifier. [23-27] However, there has been no systematic study of the electronic properties of this type of compound, as relatively few examples are known.

Oxidation of *trans*-[Pd{C≡CC≡C[Re(NO)(PPh$_3$)Cp*]}$_2$(PEt$_3$)$_2$] **1** gives a mono-cation, for which EPR studies showed that the unpaired electron is localised on one rhenium atom [28]. Electronic interaction between the two terminal ferrocenyl moieties has been found in *cis*-Ru(C≡CFc)$_2$(dppm)$_2$ and *trans*, *trans*, *trans*-Ru(C≡CFc)$_2$(CO)(L)(PBu$_3$)$_2$ [L =

CO, py, P(OMe)$_3$],[29] and in *trans*-Ru(C≡CC≡CFc)$_2$(dppe)$_2$ 2, obtained from RuCl$_2$(dppe)$_2$ and FcC≡CC≡CH in the presence of NaPF$_6$ and NEt$_3$ [30]. The cyclic voltammogram (CV) of 2 contains three reversible oxidation waves, two at -0.12 V and +0.01 V (assigned to the Fc groups) and one at +0.40 V (for the Ru^{II}/Ru^{III} system) (all redox potentials herein are referenced to the SCE). The presence of the two Fc-centred processes is consistent with there being an interaction between them through the -C$_4$-Ru-C$_4$- chain. In this complex, the Ru(dppe)$_2$ moiety (a strong electron-donating group) acts as a conductor (even possibly an amplifier), as a result of the excellent overlap which occurs between the central Ru d orbitals and the π orbitals of the C$_4$ fragments.

1

2
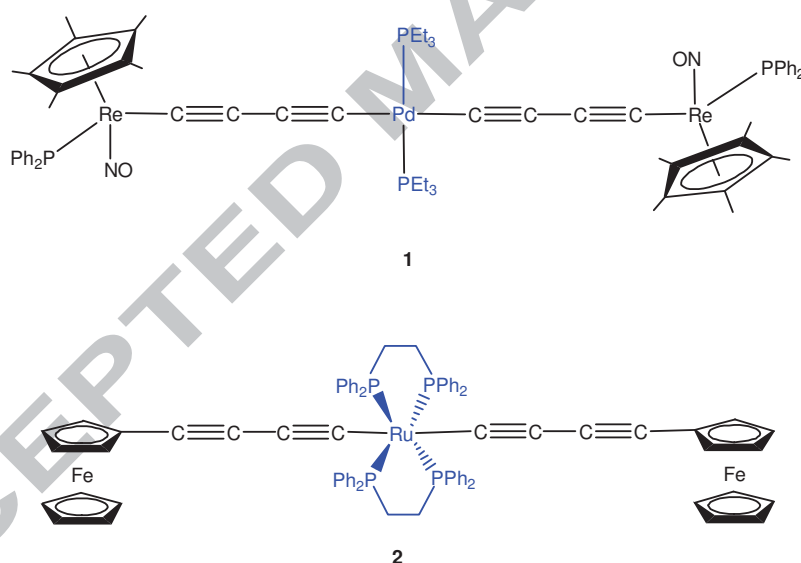
We have described the complex [Hg{C≡CC≡C[Ru(dppe)Cp*]}$_2$] **3**, obtained from [Ru(C≡CC≡CH)(dppe)Cp*] and Hg(OAc)$_2$ [31]. This was found to have an unusually bent Ru-C$_4$-Hg-C$_4$-Ru sequence [Hg-C-C 166.5(2)°], although DFT analysis of its electronic structure suggested that the bending was due to 'crystal packing forces'. Of more interest was

the finding that there is no Hg contribution to the HOMO of the model complex [Hg{C≡CC≡C[Ru(dHpe)Cp*]}$_2$] [**3-H**; dHpe = H$_2$P(CH$_2$)$_2$PH$_2$], thus precluding any electronic communication between the ruthenium termini, i.e., the Hg atom acts as an insulator. This was supported by cyclic voltammetry which showed only one 2-eoxidation process.

3
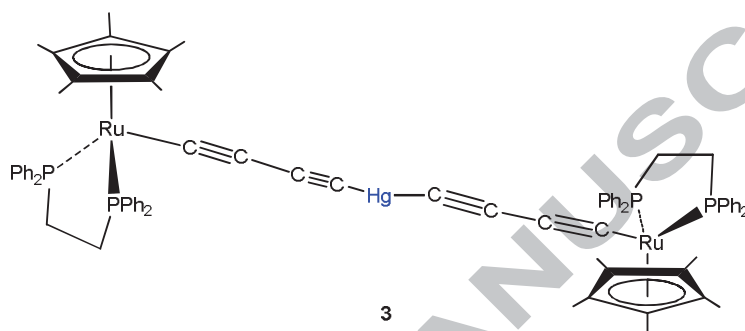
We have also reported that enhanced interaction occurs in the trimetallic complex *trans*-{Cp*(dppe)Ru}C≡CC≡C{Ru(dppe)$_2$}C≡CC≡C{Ru(dppe)Cp*} **4**, as shown by DFT calculations to be the result of efficient overlap of the C$_4$ orbitals with all metal fragments, the HOMO and HOMO-1 spanning all eleven atoms of the Ru-C$_4$-Ru-C$_4$-Ru chain [32].

4
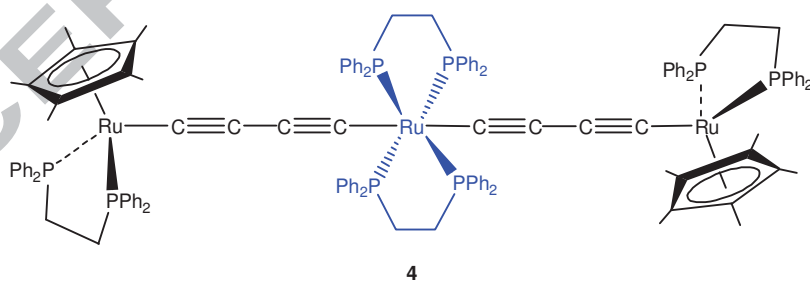
More recently, the Berke group has described the complexes {X(depe)$_2$Fe}(C≡C)$_2${Fe(depe)$_2$X} [X = (C≡C)$_n$SnMe$_3$, n = 1, 2; depe = bis(diethylphosphino)ethane], which was used to make highly conductive molecular wires. Cleavage of the SnMe$_3$ groups occurred on interaction with gold electrodes to give Au ...

$(C \equiv C)_n\{Fe(depe)_2\}(C \equiv C)_2\{Fe(depe)_2\}(C \equiv C)_n$ ... Au systems. In these, a strongly hybridised electronic system extends over the molecule-metal interfaces.[33]

There is a limited amount of information about complexes in which a polynuclear group links two diyndiyl-metal fragments. Ren's group has described complexes such as $Fc(C \equiv C)_n\{Ru_2(dmba)_4\}(C \equiv C)_n Fc$ (Fc = ferrocenyl, dmba = *N*,*N'*-dimethylbenzamidinate, n = 1-4) in which strong electronic coupling between the Fc termini exists over a distance of up to 27 Å.[34] Related studies involved $\{(Xap)_4 Ru_2\}(C \equiv C)_n\{Ru_2(dmba)_4\}(C \equiv C)_n\{Ru_2(Xap)_4\}$ [Xap = 2-(3-methoxy- or 3,5-dimethoxy-anilino)pyridinate, n = 2], where voltammetric, spectroscopic and DFT methods demonstrated extensive delocalisation over 20 Å.[35] Further examples of $Fc(C \equiv C)_n$ (n = 1, 2) linked by $Ru_3(NNN)_3$ (NNN = 2,2'-dipyridylamido),[36] $Pt_2(dppm)_2$,[37] $Pt_6(PBu^t_2)_4(CO)_4$,[38] $Cu_3(dppm)_3$,[39] or $M_6(dppm)_2$ clusters [40] are known, while a few complexes contain poly-yndiyl-metal fragments to which are bridged by $M_6(dppm)_2$ clusters [41] or complexed to $Co_2(CO)_4(L)_2$ [L_2 = $(CO)_2$, dppm] [42] or $Os_3(CO)_n$ (n = 10, 11) [43,44] groups. Reactions of $\{Cp(Ph_3P)_2Ru\}_2\{\mu-(C \equiv C)_n\}$ (n = 1, 2) with $Fe_2(CO)_9$ afford $\{Cp(Ph_3P)_2Ru\}C_m\{Fe_3(CO)_9\}C_m\{Ru(PPh_3)_2Cp\}$ (m = 3, 5, resp.).[42]

In 1993, Gimeno and co-workers reported the syntheses and crystal structures of various trinuclear alkynyl-Cu(I) complexes such as $[Cu_3(\mu\text{-}dppm)_3(\mu_3\text{-}\eta^1\text{-}C \equiv CR)_2]BF_4$ (where R = Ph, ^{t}Bu, CH_2OMe) [45]. Since then, a number of polynuclear Cu(I) and Ag(I) alkynyl complexes have been reported by Yam's group [46-48] and by others [49]. These are promising building blocks for the construction of rigid-rod oligomeric and polymeric materials and exhibit interesting properties such as luminescence and an ability to mediate electron delocalisation. They are generally obtained from the reactions of $[M_2(\mu\text{-}dppm)_2(NCMe)_n]X_2$ ([**5-M**]X_2, M = Cu, n = 4; Ag, n = 2; X = BF_4, PF_6) with a terminal alkyne in the presence of an excess of KOH or dbu in refluxing $CH_2Cl_2/MeOH$ [45]. Depending on the stoichiometry and reaction conditions, either mono- or bis-μ_3-alkynyl-Group 11 metal cluster compounds may be obtained. In some cases, further reaction may occur to give bi-, tetra- or hexa-nuclear clusters.[41,48]

6

We considered that it would be interesting to determine whether any interaction between the end-groups would occur in similar systems in which two -C≡CC≡C{Ru(dppe)Cp*} fragments (a strong electron donor) are linked by clusters $M_3(\mu$-dppm$)_3$ (M = Cu, Ag). Complexes of the general formula [{$M_3(\mu$-dppm$)_3$}{μ_3-C≡CC≡C[Ru(dppe)Cp*]}$_n$]X_{3-n} (M = Cu, Ag; n = 1, 2; X = BF$_4$, PF$_6$; Scheme 1) have now been synthesised and characterised, including single crystal X-ray studies of the n = 1 (Cu, Ag) and 2 (Cu) members. Some studies were also carried out with the diyndiyl-rhenium systems [{$M_3(\mu$-dppm$)_3$}{μ_3-C≡CC≡C[Re(CO)$_3$(Bu$^t_2$-bpy)]}$_2$]X with a view to determining any factors which may be responsible for the asymmetry found in the attachment of a diynyl group to the M_3 clusters in some complex structures.

2. Results and discussion

2.1. Ruthenium complexes.

2.1.1. Synthesis and Spectroscopy. Bright orange crystalline [{Cu$_3(\mu$-dppm$)_3$}{μ_3-C≡CC≡C[Ru(dppe)Cp*]}]X$_2$ [**6**]X$_2$ was obtained from [Ru(C≡CC≡CH)(dppe)Cp*] and [Cu$_2(\mu$-dppm$)_2$(NCMe)$_2$]X$_2$ [**5-Cu**]X$_2$ in THF / NEt$_3$ (Scheme 1; for comparative purposes, Scheme 1 shows the atom numbering scheme employed across the present compounds, as well as those derived from literature reports). Under similar conditions with [**5-Cu**](PF$_6$)$_2$, attempts to add a second ruthenium diynyl fragment failed, only [**6**](PF$_6$)$_2$ being formed, even when a large excess of the diynyl complex was used. However, by using the stronger bases KOH or dbu (1,8-diazabicyclo[5.4.0]undec-1-ene), the bis-ruthenium complex [{Cu$_3(\mu$-dppm$)_3$}{μ_3-C≡CC≡C[Ru(dppe)Cp*]}$_2$]PF$_6$ [**7**]PF$_6$ was formed, although in all cases small quantities of [**6**](PF$_6$)$_2$ were also obtained. Separation of the two complexes was readily achieved by column chromatography (alumina). The BF$_4$ salts of [**6**]$^{2+}$ and [**7**]$^+$, [**6**](BF$_4$)$_2$ and [**7**]BF$_4$, were similarly obtained from [Ru(C≡CC≡CH)(dppe)Cp*] and [**5-Cu**](BF$_4$)$_2$

7

using LiBu or dbu as a base respectively. The analogous silver(I) complexes $[\mathbf{8}](PF_6)_2$, $[\mathbf{8}](BF_4)_2$, $[\mathbf{9}]PF_6$ and $[\mathbf{9}]BF_4$ were also obtained from reactions carried out in the dark.
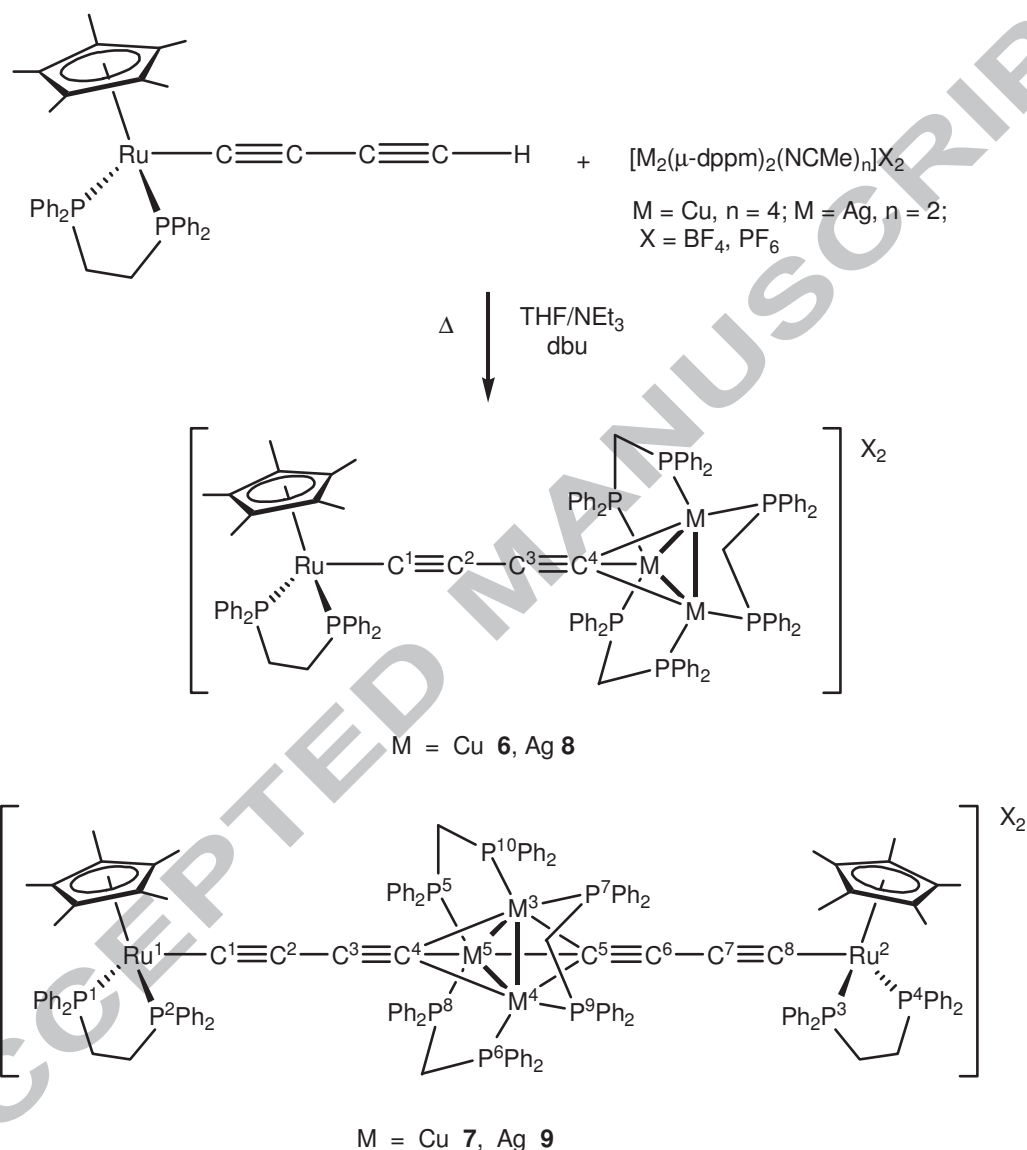
Scheme 1. Syntheses of complexes $[\mathbf{6\text{-}9}]X_2$. The global atom numbering scheme utilised in Table 2 and elsewhere for the description of these complexes is shown.

Full characterization of these compounds from elemental microanalyses and by spectroscopy was achieved. The NMR spectra contain resonances as expected for the {Ru(dppe)Cp*} and {M_3(μ-dppm)$_3$} fragments (Table 1). The mono- and bis-diyndiyl complexes could be distinguished by the relative intensities of the dppe (δ_P ca 80) and dppm [δ_P ca -7 (Cu), ca -7 to +2 (Ag)] resonances. The IR spectra of all complexes contain ν(C≡C) bands at 1983 (**6** and **8**) or between 2015 and 2033 cm^{-1} (**7** and **9**); the PF$_6$ and BF$_4$ salts are distinguished by IR bands at 838 and 1052 cm^{-1} [ν(PF) and ν(BF), respectively].

< Table 1 here >

9

Table 1. Some NMR data for complexes [{M$_3$(μ-dppm)$_3$}{μ-C≡CC≡C

[Ru(dppe)Cp*]}$_n$]$^{(3-n)+}$ [**6-9**]X$_{3-n}$

Complex			^{1}H	^{13}C	^{31}P
#	M	n			
6 / BF$_4$	Cu	1	1.67 Cp* 2.30-2.60 dppe-CH$_2$ 3.09, 3.37 dppm-CH$_2$ 6.60-7.80 Ph	10.9, 95.4 Cp* 27.2 dppm-CH$_2$ 30.5 dppe-CH$_2$ 128.0-139.0 Ph 65.6, 90.8, 116.8 C(2,3,4)	-8.9 dppm 78.7 dppe
6 / PF$_6$	Cu	1	1.77 Cp* 2.57, 2.89 dppe-CH$_2$ 3.50 dppm-CH$_2$ 7.09-7.89 Ph	10.9, 95.7 Cp* 28.6 CH$_2$ 129.0-137.9 Ph 68.1 (J_{CP} 17) C(4), 90.6, 117.8 C(2,3), 158.4 (J_{CP} 21) C(1)	-142.4 (J_{PF} 710) PF$_6$ -7.8 dppm 78.9 dppe
7 / BF$_4$	Cu	2	1.56 Cp* 2.56-2.87 dppe-CH$_2$ 3.14-3.17 dppm-CH$_2$ 6.81-7.17 Ph	11.5, 94.2 Cp* 28.0-28.2 CH$_2$ 128.0-137.1 Ph 64.8 C(4,5), 95.0, 117.2 C(2,3,6,7), 121.5 (J_{CP} 21) C(1,8)	-7.3 dppm 79.4 dppe
7 / PF$_6$	Cu	2	1.86 Cp* 2.58, 3.02 dppe-CH$_2$ 3.14 dppm-CH$_2$ 6.76-7.97 Ph	11.5, 94.2 Cp* 28.3 CH$_2$ 128.4-138.8 Ph 65.3 br C(4,5), 94.6, 118.09 C(2,3,6,7), 121.8 (J_{CP} 21) C(1,8)	-142.3 (J_{PF} 710) PF$_6$ -7.5 dppm 79.1 dppe
8 / BF$_4$	Ag	1	1.66 Cp* 2.83 dppe-CH$_2$ 3.02-4.17 dppm-CH$_2$ 6.70-8.05 Ph		2.6 (J_{PAg} 365.7) dppm 80.5 dppe
9 / BF$_4$	Ag	2	1.56 Cp* 1.79-1.87, 2.53-2.59 dppe-CH$_2$ 3.02-3.12 dppm-CH$_2$ 6.79-7.37 Ph	10.0, 94.2 Cp* 28.8-28.9 CH$_2$ 128.0-133.8 Ph 51.7 C(4,5), 95.9, 116.6 C(2,3,6,7) 123.6 C(1,8)	-1.2 dppm 80.5 dppe
9 / PF$_6$	Ag	2	1.59 Cp* 1.77-1.84, 2.21-2.55 dppe-CH$_2$ 3.22-3.25 dppm-CH$_2$ 6.87-7.90 Ph	9.8, 94.2 Cp* 28.2-28.7 CH$_2$ 127.8-133.6 Ph 51.6 C(4,5), 95.8, 116.5 C(2,3,6,7), 123.6 C(1,8)	-141.1 (J_{PF} 711) PF$_6$ -1.3 dppm 80.7 dppe

In most cases, four resonances for the atoms of the C_4 chain(s) were observed in the ^{13}C NMR spectra, although the anticipated couplings were not always resolved. In [**7**]$^+$, a triplet at δ 121 [J_{CP} = 21 Hz] is assigned to C(1,8), although J_{CP} is not resolved in the similar signal at δ ca 123 in [**9**]$^+$. A significant down-field shift occurs for C(1) in [**6**]$^{2+}$, which resonates at δ 158 [J_{CP} = 21 Hz]. This is accompanied by a well-resolved septet at δ 68.12 [J_{CP} = 17 Hz], coupling to the six dppm-P nuclei being found, thus allowing this signal to be assigned to C(4). In the Ag complexes, this resonance is found downfield at δ ca 51. Resonances for C(2,3) [and for C(6,7) if present] cannot be assigned unequivocally, but are found at δ ca 90-96 and 117. In [**8**]BF$_4$, the ^{31}P dppm resonance appears as a well-resolved septet with J_{PAg} = 365.7 Hz.

At low exit-voltage (80 V), the electrospray-ionisation mass spectrum (ESI-MS) of [**8**](BF$_4$)$_2$ contained [**8**$^{2+}$ + BF$_4^-$]$^+$, [**8**]$^{2+}$ and [Ag$_2$(dppm)$_2$]$^{2+}$ at m/z 2247, 1080 and 492, respectively, the compositions being confirmed by high resolution mass measurements. Further fragmentation occurs at a higher exit-voltage (150 V), when ions corresponding to [Ag$_2$(dppm)Ru(C$_4$)(dppe)Cp*]$^+$ (m/z 1283), [Ag$_3$(dppm)$_2$Ru(C$_4$)(dppe)Cp*]$^{2+}$ (888), [Ag(dppm)$_2$]$^+$ (877) and [Ag(dppm)]$^+$ (491) are also present.

2.1.2. Crystal Structures. The molecular structures of the complexes [**6**](BF$_4$)$_2$, [**7**](PF$_6$) and [**8**](BF$_4$)$_2$ (orthorhombic and triclinic)(all solvated) have been determined. That of [**7**](PF$_6$) confirms the expected structure with the -C≡CC≡C[Ru(dppe)Cp*] groups linked via the {Cu$_3$(μ-dppm)$_3$} moiety. The cation (Fig. 1) is nearly linear with some asymmetry in the attachment of one of the -C≡CC≡C[Ru(dppe)Cp*] groups (see below for further discussion). The coordination environment of the Ru(dppe)Cp* end groups is typical with the one group rotated along the [Ru]-{Cu$_3$(μ-dppm)$_3$} centroid-[Ru] axis by ca 90° with respect to the other.

11

This appears to be a consequence of the disposition of the dppm ligands about the central

{Cu$_3$(μ-dppm)$_3$} cluster.

< Fig. 1 here >
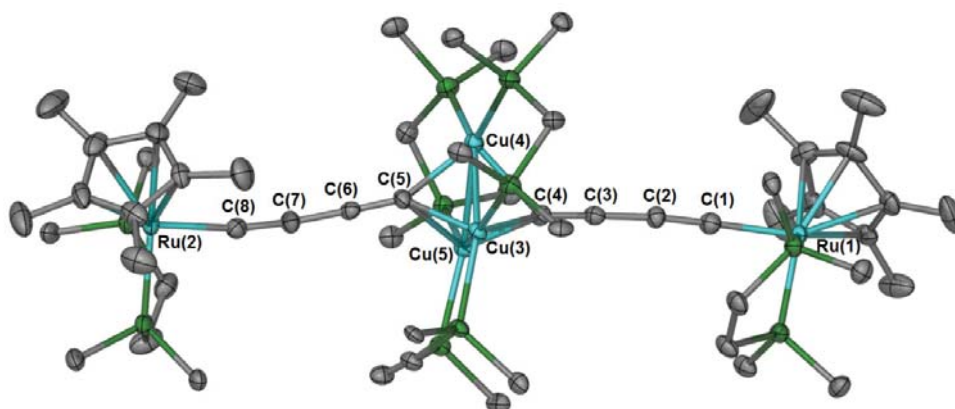
Fig. 1. A representation of the molecular structure of [{Cu$_3$(μ-dppm)$_3$}{μ_3-C≡CC≡C[Ru(dppe)Cp*]}$_2$]PF$_6$[**7**]PF$_6$. Ellipsoids have been drawn at the 50% probability level with solvate molecules, the anion, hydrogen atoms and the phenyl carbons of the dppe and dppm ligands (except the *ipso*-carbons) omitted for clarity.

The structures of [**6**,**8**](BF$_4$)$_2$·nS are very similar, being isomorphous (orthorhombic), with cation **8** further exemplified in the more precise determination of the triclinic THF solvate of [**8**](BF$_4$)$_2$ [which offers more precise distances within the diynyl string (Table 2)] as presented in Fig. 2. The solvent contents of the lattices of orthorhombic [**6**,**8**](BF$_4$)$_2$, probably acetone, are ill-defined; for each of the four present structures a single formula unit, devoid of crystallographic symmetry, comprises the asymmetric unit. Comparative core geometries for the cations are given in Table 2. Fig. 2 presents representative plots of the cations of [**7**]$^+$ and [**8**]$^{2+}$, in particular highlighting the disposition of the diynyl group(s) around the {M$_3$(μ-dppm)$_3$} cluster.

Note in (a) the difference in bonding (μ$_2$ cf. μ$_3$) of the two diynyl ligands [but an average of C(4)-Cu and C(8)-Cu in **7** gives 2.185 and 2.176 Å, respectively], and in (c) the interaction of the BF$_4$anion with the Ag$_3$ cluster[absent in (b)]. In all structural projections, the unique dppmligands (see below) lie to the left of the figure, with their 'U' methylene groups directed toward the reader in projection (i), and towards the quasi-mirror plane of the core in the plane of the page in (ii). Where phenyl and methylene hydrogen atoms are involved in close intramolecular contacts, these are shown.

< Fig. 2 here >

< Table 2 here >

14
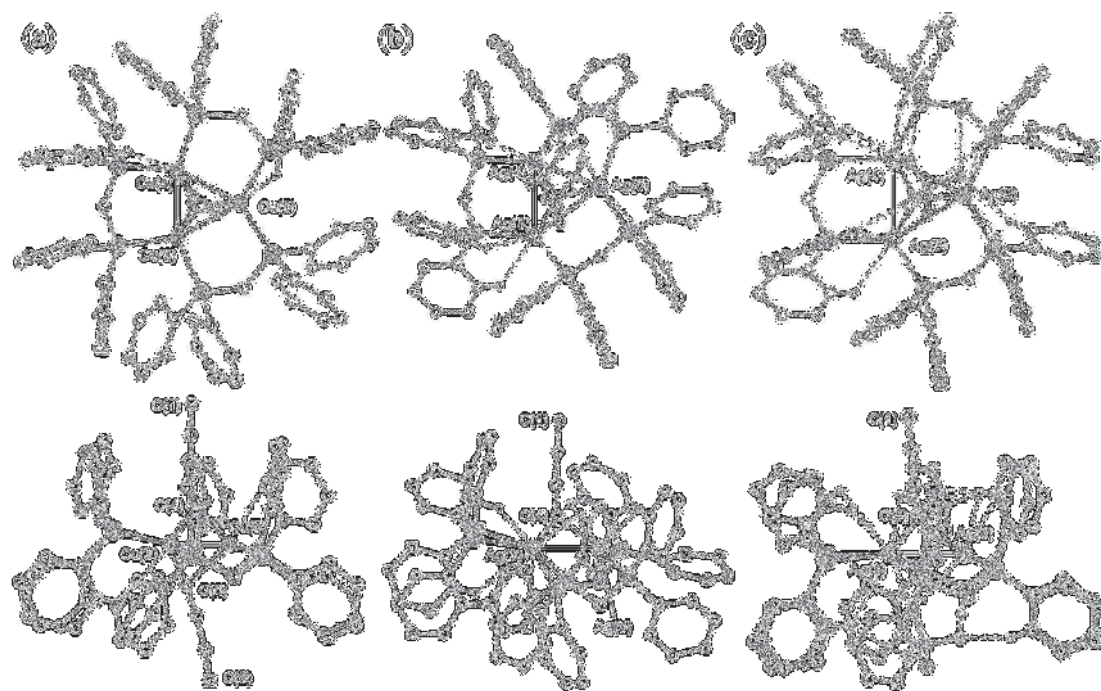
Fig. 2. Projections of the cations in (a) [{Cu$_3$(μ-dppm)$_3$}{C≡CC≡C[Ru(dppe)Cp*]}$_2$]PF$_6$ [**7**]PF$_6$ (i) normal to and (ii) through the Cu$_3$ plane, the latter displaying the two bridging modes (μ$_2$ and μ$_3$) of the diynyl ligand within the one species.   (b) and (c)   [{Ag$_3$(μ-dppm)$_3$}{μ$_3$-C≡CC≡C[Ru(dppe)Cp*]}](BF$_4$)$_2$ [**8**](BF$_4$)$_2$ [acetone (orthorhombic) and THF solvates (triclinic)] similarly.

Table 2. Selected core geometries for the cations of $[\{M_3(\mu\text{-dppm})_3\}\{\mu_3\text{-C}\equiv CC\equiv C$ $[Ru(dppe)Cp^*]\}](BF_4)_2$ [M = Cu, [**6**](BF$_4$)$_2$; Ag, [**8**](BF$_4$)$_2$ (two forms: *Pbca*, $P\bar{1}$)] and $[Cu_3(\mu\text{-dppm})_3\{\mu_3\text{-C}\equiv CC\equiv C[Ru(dppe)Cp^*]\}_2](PF_6)$ [**7**]PF$_6$.Main DFT optimized data (obtained on models, see computational details) are given in brackets.

Compound	[**6**](BF$_4$)$_2$(M = Cu) (*Pbca*)	[**8**](BF$_4$)$_2$(M = Ag) (*Pbca*; $P\bar{1}$ *)	[**7**]PF$_6$ (M = Cu) (*P2$_1$/n*)
Bond lengths (Å)			
Ru(1)-P(dppe); Ru(2)-P(dppe)	2.275, 2.277(2)	2.265, 2.277(5) *2.276(1), 2.276(2)*	2.253, 2.249(2); 2.239, 2.276(2)
Ru-C(cp)	2.213-2.297(9)	2.15-2.30(2) *2.244-2.293(5)*	2.232-2.254(6); 2.221-2.292(6)
(av.)	2.25	2.22 *2.265*	2.243; 2.257
Ru(1)-C(1); Ru(2)-C(8)	1.937(8) [1.958]	1.76(2) *1.979(5)* [1.970]	2.006(6); 1.999(6) [1.941 x 2]
C(1)-C(2); C(7)-C(8)	1.25(1) [1.265]	1.33(2) *1.232(7)* [1.261]	1.228(8); 1.218(8) [1.251 x 2]
C(2)-C(3); C(6)-C(7)	1.36(1) [1.323]	1.39(2) *1.361(7)* [1.333]	1.386(8); 1.367(8) [1.346 x 2]
C(3)-C(4); C(5)-C(6)	1.22(1) [1.286]	1.32(2) *1.226(7)* [1.277]	1.207(8); 1.220(8) [1.261 x 2]
C(4)-M(3,4,5); C(5)-M(3,4,5)	2.048(7), 2.021(7), 2.041(8) [2.008 x 2], [2.016]	2.27(1), 2.20(1), 2.17(2) *2.259(4), 2.236(5), 2.259(5)* [2.268 x 2], [2.265]	2.230(5), 2.225(6), 2.100(6); 2.130(6), 2.082(6), 2.316(6) [2.107 x 2], [2.174 x 4]
M(3)-M(4,5)	3.052, 2.837(1) [3.032 x 2]	3.353, 3.061(2) *3.2106(5), 3.0744(6)* [3.391 x 2]	2.508(1), 2.648(1) [2.615 x 2]
M(4)-M(5)	2.558(1) [3.034]	2.870(2) *3.0657(6)* [3.421]	2.617(1) [2.624]
M(3)-P(dppm)	2.281, 2.247(2)	2.489, 2.440(4) *2.462(1), 2.467(1)*	2.270(2), 2.267(2)
M(4)-P(dppm)	2.262, 2.239(1)	2.465, 2.441(4)	2.251(2), 2.255(2)

		2.461(1), 2.467(1)	
M(5)-P(dppm)	2.246, 2.277(1)	2.390, 2.444(4)	2.298(2), 2.280(2)
		2.460(1), 2.474(1)	
Bond angles (°)			
Ru(1)-C(1)-C(2); Ru(2)-C(8)-C(7)	176.0(7)	169.1(1) *175.6(4)*	178.9(6); 165.9(5)
C(1)-C(2)-C(3); C(6)-C(7)-C(8)	177.2(9)	177.5(1) *178.6(5)*	175.0(7); 171.5(6)
C(2)-C(3)-C(4); C(5)-C(6)-C(7)	178.4(8)	175.0(1) *179.6(6)*	178.4(7); 175.9(6)
C(3)-C(4)-M(3,4,5); C(6)-C(5)-M(3,4,5)	113.6, 127.3, 140.9(6)	108.5, 130.1, 139.4(1) *121.7(4), 131.6(4), 127.0(4)*	133.3(5), 132.7(5), 142.8(5); 138.2(5), 148.6(5), 113.7(4)

* In the $P\bar{1}$ form (values in italics), one of the anions has a close approach to the side of the M$_3$ triangle.

2.1.3.Electrochemistry. The cyclic voltammograms (CVs) of the complexes [{M$_3$(μ-dppm)$_3$}{(μ$_3$-C≡CC≡C)[Ru(dppe)Cp*]}$_2$]X (M = Cu [**7**]$^+$, Ag [**9**]$^+$; X = PF$_6$, BF$_4$) were measured in CH$_2$Cl$_2$ under similar conditions. The CVs appear not to be diffusion controlled and show two quasi-reversible 1-e oxidation waves, with potentials essentially the same, only small differences between the two salts being found (Fig. 3, Table 3).

< Figure 3 here >

< Table 3 here >
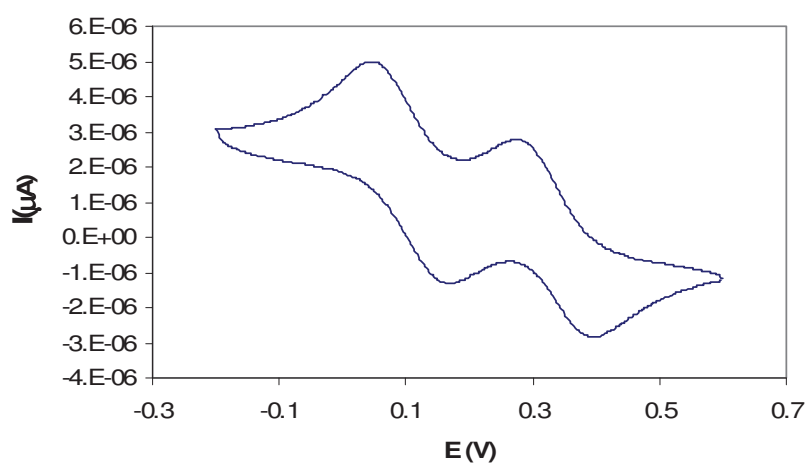
Fig. 3. Cyclic voltammogram of [**7**]BF$_4$.

Table 3. Electrochemical data for complexes **7** and **9**

Complex	E$_1$ / V	E$_2$ / V	ΔE$_{12}$ / V
7 / PF$_6$	+0.15	+0.36	0.23
7 / BF$_4$	+0.17	+0.39	0.23
9 / PF$_6$	+0.26	+0.43	0.16
9 / BF$_4$	+0.29	+0.46	0.17
{Cp*(dppe)Ru}$_2$C$_4$[a]	-0.43	+0.22	0.65
{Cp*(dppe)Ru}$_2$C$_8$[b]	+0.08	+0.43	0.35

[a]E_3 +1.04, E_4 +1.54 (irr.) V. [b]E_3 +1.07, E_4 +1.27 V. All values *vs* SCE.

Values of E_1 and E_2 are considerably larger than those of either {Ru(dppe)Cp*}$_2$(μ-C$_n$) (n = 4, 8), showing that insertion of the M$_3$(dppm)$_3$ cluster makes the complexes generally more difficult to oxidise than analogues containing only carbon chains linking the two redox centres. While the separation of the first two waves (ΔE_{12}) is often considered to be an indication of the extent of interactions between the two redox centres,[50,51] this assessment cannot be reliably made in the absence of other measurements. Several studies have shown that ΔE values are significantly affected by other factors, such as the medium used in the determination,[52] counter-ions present,[52,53] metal-metal electronic coupling (where closely spaced waves may result when the different oxidation states have similar stabilities),[53,54] conformational effects,[13c] and electrostatic and magnetic effects. This area has recently been reviewed.[52a,55-57]

Values of ΔE_{12} for [7]BF$_4$ and [9]BF$_4$ are 220 and 160 mV, respectively, i.e., they are within the cross-over area for Robin-Day Class II / Class III complexes, which is often considered to be around 200 mV.[50] These values are significantly lower than the values of 650 and 350 mV, respectively, for {Ru(dppe)Cp*}$_2$(μ-C$_n$) (n = 4, 8) [41] and 380 mV for **4**.[32] Thus, it may be concluded that the insertion of the trinuclear Group 11 cluster between the two diyndiyl fragments allows some electronic interaction between the metal termini to be maintained. More detailed studies, including spectroscopic methods, are necessary to delineate the reasons for these differences.

2.1.4. DFT calculations. In order to obtain some insight into possible reasons for these findings, density-functional theory (DFT) calculations have been carried out on the model cationic clusters [{M$_3$(μ-dHpm)$_3$}{μ$_3$-C≡CC≡C[Ru(dHpe)Cp*]}$_2$]$^+$ (M = Cu [**7-H**]$^+$, Ag [**9-H**]$^+$)of C_s symmetry where the dppm, dppe and Cp* ligands have been replaced by the dHpm,

20

dHpe and Cp ligands to reduce computational demands (see Experimental section for computational details).Results were compared and contrasted with those obtained for the mono-diynyl parent model compounds [{$M_3(\mu$-dHpm)$_3$}{μ_3-C≡CC≡C[Ru(dHpe)Cp*]}]$^{2+}$ (M = Cu [6-H]$^{2+}$ Ag [8-H]$^{2+}$).

Pertinent optimised metrical data are given in Table 2 for models 6-H, 7-H and 8-H and compared to the experimental values. The agreement is moderately satisfactory probably due to the level of theory used (C_s symmetry imposed) as well as the relatively poor quality of some of the X-ray structures. Nevertheless, as observed experimentally a comparison between 6-H and 8-H for instance shows similar Ru-C and C-C bond lengths, but C-Cu distances longer and more unsymmetrical in the bis-diynyl complex than in the mono-diynyl one. On the other hand, the Cu-Cu contacts are on average shorter in the former than in the latter. Indeed, it has been shown that there are "soft" bonding interactions between the d^{10} metal centres in these systems, which results from a mixing of vacant s/p orbitals into occupied d combinations [58,59] and / or dispersion forces.[58-61] This leads to some possible geometrical flexibility in the M_3C_2 core which can be readily influenced by crystal packing (compare the same compound within *Pbca* and *P*$\bar{1}$ symmetries in Table 2 for instance).

It was found that there are large energy gaps between the HOMO and the LUMO (of 2.32 eV and 2.29 eV for the Cu(I) and the Ag(I) complexes [7-H]$^+$ and [9-H]$^+$, respectively (Fig. 3), for a count of 46 cluster valence electrons (cve). Smaller HOMO-LUMO gaps are computed for the related 44-cve molecules (1.56 and 1.77 eV for [6-H]$^{2+}$ and [8-H]$^{2+}$, respectively). Furthermore, contour plots of the HOMO and HOMO-1 orbitals of [7-H]$^+$ (Fig. 4; similar results were obtained for [9-H]$^+$), which are almost degenerate in energy, show that these orbitals are delocalised over the entire Ru-C$_4$-Cu$_3$-C$_4$-Ru chain with a substantial contribution of the central Cu$_3$ triangle (22% Ru, 57% C8 and 13% Cu$_3$ for the

21

HOMO and 29% Ru, 56% C8 and 8% Cu_3 for the HOMO-1). This suggests that there should be some communication between the ruthenium end-groups across the Cu(I) and Ag(I) clusters, and that the two oxidation waves observed in the CVs of [**7**]PF_6 and [**9**]PF_6 correspond to loss of two electrons from the HOMO 49a″ or the HOMO-1 48a″ (singlet dication) or of one electron from both (triplet dication). Interestingly, the singlet and triplet states of [**7-H**]$^{3+}$ are very close in energy (7 kJ mol^{-1} in favour of the former).

< Fig. 4 here >
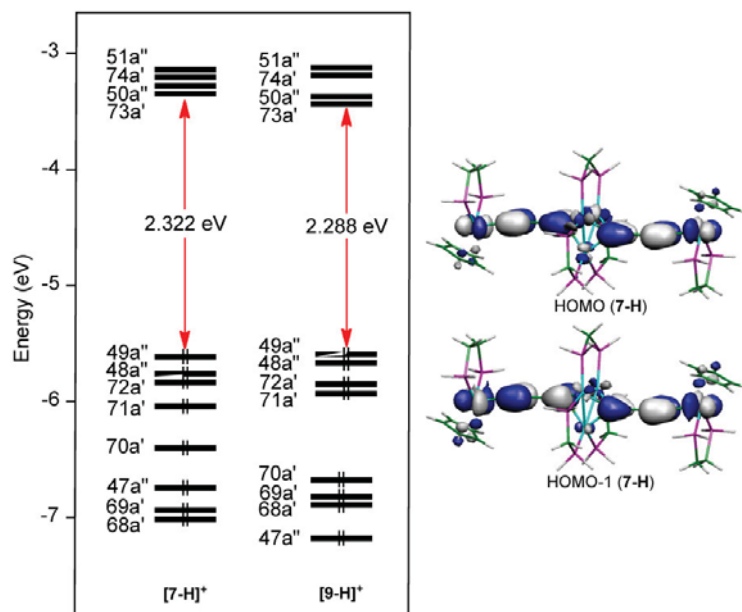
Fig. 4. Partial DFT molecular orbital diagrams for [**7-H**]$^+$(left) and [**9-H**]$^+$ (right) and contour

plots of the HOMO (upper) and the HOMO-1 (lower) of the model complex [**7-H**]$^+$ (contour

values are ±0.03 [e/bohr^3]$^{\frac{1}{2}}$).

2.2. Rhenium complexes

Yam and coworkers have described reactions between $[M_2(dppm)_2(NCMe)_2]X_2$ and $Re(C{\equiv}CC{\equiv}CH)(CO)_3(NN)$ under various conditions to give complexes of the types $[M_3(dppm)_3\{C{\equiv}CC{\equiv}C[Re(CO)_3(NN)]\}_2]PF_6$ [M = Cu, NN = bpy, Me_2-bpy (**13**), Bu^t_2-bpy [**10**]$^+$; M = Ag, NN = bpy (**14**)] [46c], and $[Ag_6(dppm)_4\{C{\equiv}CC{\equiv}C[Re(CO)_3(NN)]\}](PF_6)_2$ (NN = Me_2-bpy, Bu^t_2-bpy [**12**]$^{2+}$, phen, Br_2-phen) [48], several examples of which have been characterised by X-ray structural studies. While the Cu_3-Me_2-bpy derivative has the usual relatively symmetric attachment of the diynyl C(1) to the Cu_3 cluster [Cu(1,2,3)-C(1) = 2.064-2.290 Å; the corresponding ones in **14** are between 2.082 and 2.316 Å, see Table 2], the Ag_3-bpy analogue, which contains two different independent molecules display an unusual asymmetric arrangement of one of the diynyl carbons to the Ag_3 cluster with Ag-C distances ranging from 2.140 to 3.170 Å) [46c]. Although the X-ray determination is not very accurate (some C-C bond lengths are abnormally short), it turns out the difference in carbon-metal triangle bonding is puzzling.

$[M_3(dppm)_3\{C{\equiv}CC{\equiv}C[Re(CO)_3(NN)]\}_2]PF_6$ M = Cu, Ag; **10** M = Cu, NN = Bu^t_2-bpy
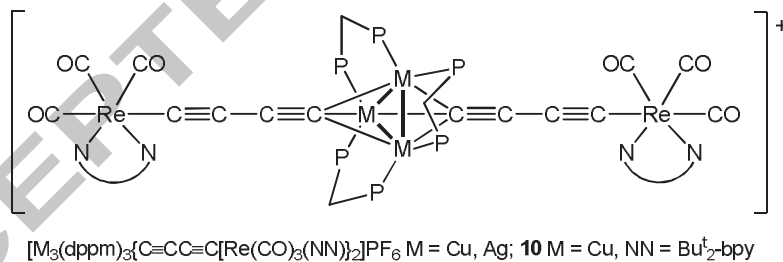
Our overall interest in this type of molecule as indicated in this paper prompted us to search for any reasons for this difference between the Cu and Ag analogues. DFT calculations on models derived from **14** suggested that, without any constraint, the asymmetric form was considerably less stable than the symmetric form, regardless of the metal. In other words, the ethynyl carbon atom seems to prefer to bind to the three metal atoms in a rather symmetrical fashion. Consequently, we have carried out some further

24

studies of this system with complexes containing the Bu^t_2-bpy ligand. No X-ray structure of the Cu_3 derivative was reported by Yam et al. [46c].

2.2.1. Structural studies. The Cu_3 complex $[Cu_3(\mu\text{-dppm})_3\{\mu_3\text{-C}\equiv CC\equiv C[Re(CO)_3(Bu^t_2\text{-bpy})\}_2]\}]PF_6$ [**10**]PF_6 was readily prepared using the same approach as described by Yam and coworkers.[46c] The X-ray structure reveals the expected Cu_3 cluster supporting two diynyl ligands, but in contrast to what is observed for **13** (where NN = Me_2-bpy), one of these is asymmetrically attached, with two Cu-C(1) [C(1')] distances of 2.088(9), 2.126(8) [2.029(8), 2.154(8)] Å, and one somewhat longer at 2.479(8) [2.324(8)] Å (Fig. 5, Table 4). The Cu-Cu distances within the $Cu_3(dppm)_3$ moiety are 2.6012(12), 2.7183(14) and 2.5539(13) Å. This distortion is further evidenced by the [Re]-C$\equiv$CC$\equiv$*C*-[Cu_3-centroid] angles which are 157.6° [144.2]°, for Re(1) and Re(2) respectively. The P-CH_2-P moiety of one dppm ligand is directed toward each Re centre with the P atoms of the third dppm close to the plane of the Cu_3 moiety [although the CH_2 is directed toward Re(1)]. Importantly, the cavity generated by the asymmetric attachment of the Re(2) end accommodates a fully occupied CH_2Cl_2 solvate molecule.

< Fig. 5 here >

< Table 4 here >

25
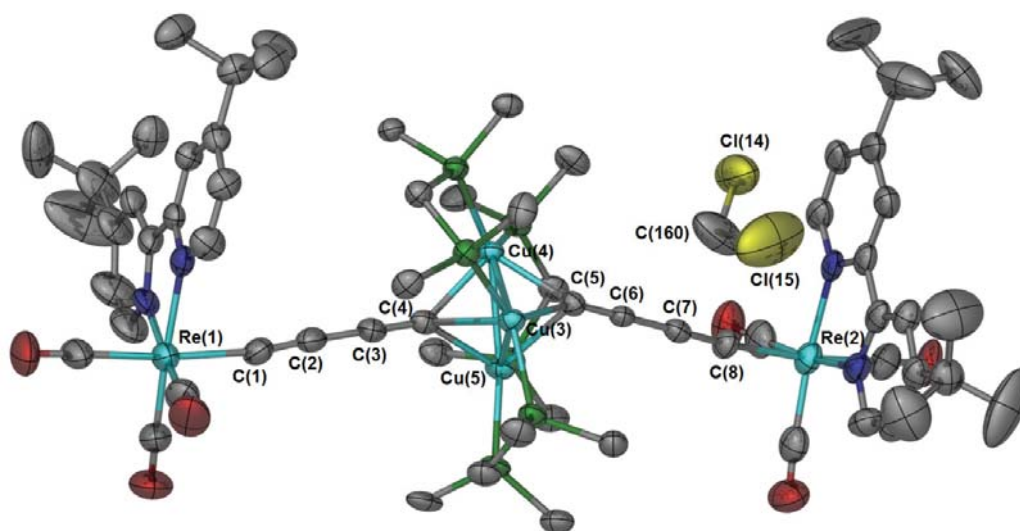
Fig. 5. A representation of the molecular structure of $[Cu_3(\mu\text{-dppm})_3\{\mu_3\text{-}C{\equiv}CC{\equiv}C[Re(CO)_3(Bu^t_2\text{-bpy})]\}_2]\}]PF_6$ [**10**]PF_6 showing the solvate CH_2Cl_2 molecule located between the $Cu_3(dppm)_3$ cluster and the $Re(CO)_3(Bu^t_2\text{-bpy})$ capping moiety. Ellipsoids have been drawn at the 50% probability level with remaining solvate molecules, the anion, hydrogen atoms and the phenyl carbons of the dppm ligands (except the *ipso*-carbons) omitted for clarity.

Table 4. Selected core geometries for the cations of $[M_3(\mu\text{-dppm})_3\{\mu_3\text{-C}\equiv\text{CC}\equiv\text{C}[Re(CO)_3(NN)]\}_2]PF_6$ (M = Cu, NN = Me_2-bpy, Bu^t_2-bpy [10]PF₆; M = Ag, NN = bpy), $[Ag_3(\mu\text{-dppm})_3(\mu\text{-Cl})\{\mu_3\text{-C}\equiv\text{CC}\equiv\text{C}[Re(CO)_3(Bu^t_2\text{-bpy})]\}]PF_6$ [11]PF₆ and $[Ag_3(\mu\text{-dppm})_3(\mu_3\text{-Cl})_2]PF_6$.

Compound	13	14*	[10]PF₆†	[11]PF₆†	[Ag₃(μ-dppm)₃Cl₂]PF₆†
	M = Cu; NN = Me₂bpy	M = Ag; NN = bpy	M = Cu; NN = Buᵗ₂-bpy	M = Ag; NN = Buᵗ₂-bpy	
Bond length (Å)					
M1-M2, M4-M5	2.659(2)	2.898(3), 2.869(3)	Cu3-Cu4 2.601(1)	Ag2-Ag3 3.034(4)	Ag1-Ag2 3.501(1)
M1-M3, M4-M6	2.574(2)	3.020(3), 2.904(3)	Cu3-Cu5 2.718(1)	Ag2-Ag4 3.277(5)	Ag1-Ag3 3.321(1)
M2-M3, M5-M6	2.553(2)	2.914(3), 3.071(3)	Cu4-Cu5 2.554(1)	Ag3-Ag4 3.077(4)	Ag2-Ag3 3.391(1)
M1-C1, M4-C1	2.290	2.747, 2.358	Cu3-C4 2.479(8)	Ag2-C42.250(4)	
M2-C1, M5-C1	2.099	2.426, 2.114	Cu4-C4 2.126(8)	Ag3-C42.319(4)	
M3-C1, M6-C1	2.154	2.215, 3.071	Cu5-C4 2.088(9)	Ag4-C42.383(4)	
M1-C1', M4-C1'	2.064	2.328, 2.411	Cu3-C5 2.029(8)		
M2-C1', M5-C1'	2.276	2.503, 3.170	Cu4-C5 2.154(8)		
M3-C1', M6-C1'	2.206	2.741, 2.140	Cu5-C5 2.324(8)		
M1-X					Ag1-Cl 2.75511(19), 2.745(2)
M2-X				Ag3-Cl5A 2.712(1)	Ag2-Cl 2.738(2), 2.7942(19)
M3-X				Ag4-Cl5A 2.737(1)	Ag3-Cl 2.706(2), 2.766(2)

* Bond lengths for both independent molecules are given, with the second showing more significant distortion.

† Due to a slightly different numbering format to the literature structures the atoms involved in the bonding under consideration are specified in the Table.

28

The silver system proved to be more complex, the reaction between [Ag$_2$(μ-dppm)$_2$(NCMe)$_2$](PF$_6$)$_2$ and Re(C≡CC≡CH)(CO)$_3$(Bu$^t_2$-bpy) being carried out in MeOH / CH$_2$Cl$_2$ and affording the mono-diynyl complex [Ag$_3$(μ-dppm)$_3$(μ-Cl)(μ_3-C≡CC≡C[Re(CO)$_3$(Bu$^t_2$-bpy)]]}]PF$_6$ [**11**]PF$_6$, characterised by ESI-MS and a crystal structure (Fig. 6, Table 4). In contrast to the structure of the Cu$_3$ complex above, however, there is a solvent molecule (refining as a disordered ethanol molecule) interacting with Cl(5A) and Ag(4) and causing the lengthening of the Ag(4)...C(4) separation to 2.383(4) Å [Ag(2,3)-C(4) 2.250(4), 2.319(4) Å]. For comparison to Cu$_3$ complex, the [Re]-C≡CC≡*C*-[Ag$_3$-centroid] angle is 173.0°, indicating a more symmetric arrangement of the Re centre of the face of the Ag$_3$ complex. On the opposing face the Cl is disordered over two sites with a 0.8:0.2 ratio established by trial refinement; the major occupancy site μ_2-Cl(5A) is coordinated by Ag(3) and Ag(4) [2.712(1) and 2.737(1) Å] and hydrogen bonding to the ethanol solvate. The non-bonding Ag(2)-Cl(5A) distance is 3.84 Å. The minor occupancy μ_2-Cl(5B) is still asymmetrically bound but more centred with respect to the Ag$_3$(dppm)$_3$ entity with bonding Ag(3) and Ag(4) distances of 2.894(5) and 2.890(6) Å and a non-bonding Ag(2)-Cl(5B) distance of 3.20 Å.

< Fig. 6 here >
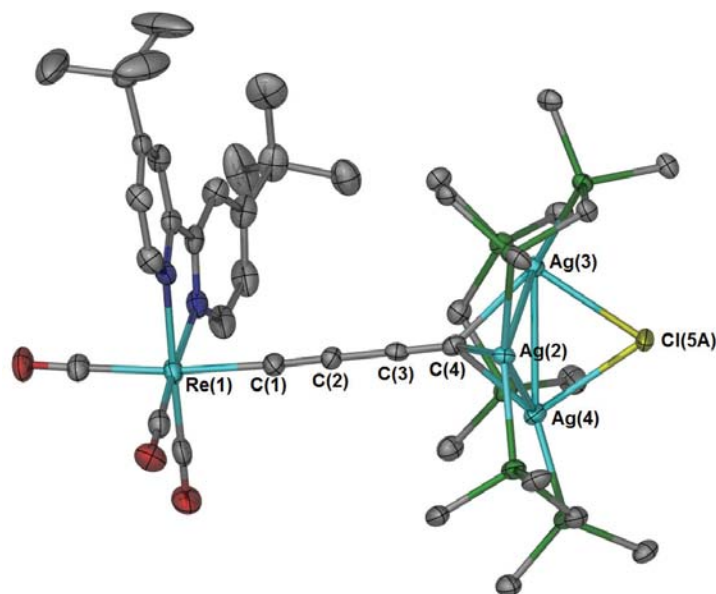
Fig. 6. A representation of the molecular structure of $[Ag_3(\mu\text{-dppm})_3(\mu_2\text{-Cl})\{\mu_3\text{-}C{\equiv}CC{\equiv}C[Re(CO)_3(Bu^t_2\text{-bpy})]\}]PF_6$ [**11**]PF_6. Ellipsoids have been drawn at the 50% probability level with solvate molecules, the anion, hydrogen atoms and the phenyl carbons of the dppm ligands (except the *ipso*-carbons) omitted for clarity. Only the major occupancy position (0.8) of the asymmetrically coordinated Cl ligand is shown.

We have been unable to obtain $[Ag_3(dppm)_3\{C{\equiv}CC{\equiv}C[Re(CO)_3(Bu^t_2\text{-}bpy)]\}_2]PF_6$ to carry out a comparative structural determination; a minor product was identified as known $[Ag_3(\mu\text{-}dppm)_3Cl_2]PF_6$ by ESI-MS and from an X-ray structure. This complex has the Cl ligands symmetrically coordinated to the $Ag_3(dppm)_3$ entity (Table 4).

Further studies afforded the crystallographically characterised hexa-silver cluster $[Ag_6(\mu\text{-}dppm)_4\{C{\equiv}CC{\equiv}C[Re(CO)_3(Bu^t_2\text{-}bpy)]\}_4](PF_6)_2$ **[12]**$(PF_6)_2$, reported earlier by Yam et al. [48], and directly related to the analogous crystallographically characterised Me_2-bpy derivative (see SI Figure 1 for representations of the structure). Due to the additional steric bulk of the Bu^t_2-bpy ligands coordinated at Re, $[Ag_6(\mu\text{-}dppm)_4\{C{\equiv}CC{\equiv}C[Re(CO)_3(Bu^t_2\text{-}bpy)]\}_4](PF_6)_2$ crystallises in a different space group but the cation has a very similar structure to that of the Me_2-bpy derivative. The central $Ag_6(dppm)_4$ cluster has a flattened tetrahedral arrangement of four Ag centres (Ag5, Ag6, Ag7, Ag9) with Ag8 and Ag10 bonded along opposite edges to Ag5 / Ag9 and Ag6 / Ag7, respectively. The Ag-Ag bond lengths are in the range 2.9174(12) - 3.0291(11) Å [one longer interaction, 3.2495(15) Å, exists between Ag5 and Ag9 as part of the distorted tetrahedron]; these are shorter than the sum of van der Waals radii for Ag (3.4 Å) [50] and supportive of weak Ag ··· Ag interactions. Two dppm ligands coordinate both Ag8 and Ag10, while one P donor contributes to the coordination environment of the central Ag atoms. Each butadiynyl group binds into the diamond-shaped faces within the Ag_6 core and is coordinated to three silver atoms in a μ_3,η^1-bridging mode [Ag-C distances in the range 2.207(10) – 2.79(1) Å]. The four butadiynyl groups are capped at the other ends by the $Re(CO)_3(Bu^t_2$-bpy) moiety.

3. Conclusions

Syntheses of Cu(I) and Ag(I) diynyl-Ru complexes of general formula [{M$_3$(μ-dppm)$_3$}{μ$_3$-C≡CC≡C[Ru(dppe)Cp*]}$_n$]X$_{3-n}$ (M = Cu, n = 1 [**6**]X$_2$, 2 [**7**]X; M = Ag, n = 1 [**8**]X$_2$, 2 [**9**]X; X = BF$_4$, PF$_6$) were successfully achieved. Cyclic voltammetric studies supported by DFT calculations suggest that electronic interaction between the two ruthenium centres in {Ru(dppe)Cp*}$_2$(μ-C$_8$) is significantly weakened when a trinuclear Cu(I) or a Ag(I) cluster is inserted into the carbon chain, resulting from considerably weaker overlap between the carbon chains and the M$_3$(μ-dppm)$_3$ cluster. The presence of one or two diynyl ligands exercises a significant influence over the geometry of the trinuclear cation core. With only one ligand, and a feebly bound or non-existent donor to the other face, agostic interactions between dppm hydrogen atoms and the M$_3$ core may produce unusual conformational changes in the dppm chelate rings, as discussed elsewhere.[62].

In the rhenium system, the complexes [Cu$_3$(μ-dppm)$_3${μ$_3$-C≡CC≡C[Re(CO)$_3$(Bu$^t_2$-bpy)]}$_2$]PF$_6$ [**10**]PF$_6$, [Ag$_3$(μ-dppm)$_3$(Cl){μ$_3$-C≡CC≡C[Re(CO)$_3$(Bu$^t_2$-bpy)]}]PF$_6$ [**11**]PF$_6$ and [Ag$_6$(μ-dppm)$_4${C≡CC≡C[Re(CO)$_3$(Bu$^t_2$-bpy)]}$_4$](PF$_6$)$_2$ [**12**](PF$_6$)$_2$ have been obtained from **5** and Re(C≡CC≡CH)(CO)$_3$(Bu$^t_2$-bpy).[46c,48] As shown in Tables 2 and 4, there are two shorter and one longer M-M separations in the M$_3$ clusters of the bis-diynyl complexes. We have drawn attention to the asymmetric diynyl ligand found in the crystal of the Ag$_3$ complex above. Theoretical calculations suggest that this conformer is significantly unstable with reference to the symmetrical form. However, in the X-ray structure, there does not appear to be any other molecule within the coordination sphere of the Ag$_3$ cluster which might be responsible for partial loosening of the diynyl-Ag$_3$ bonding. This result further suggests that the C(1)-M bond is relatively weak, ready displacement of one M atom occurring by

32

interaction with appropriate solvate molecule(s). We note that the $M_3(dppm)_3$ cluster is resistant to dissociation under these conditions.

4. Experimental

4.1. *General Experimental Details.* All reactions were carried out under dry nitrogen, although normally no special precautions to exclude air were taken during subsequent work-up. Common solvents were dried, distilled under nitrogen and degassed before use. Separations were carried out by preparative thin-layer chromatography on glass plates (20 x 20 cm^2) coated with silica gel (Merck 60 GF254, 0.5 mm thick).

Instruments. IR spectra were obtained on a Bruker IFS28 FT-IR spectrometer. Spectra in CH_2Cl_2 were obtained using a 0.5 mm path-length solution cell with NaCl windows. Nujol mull spectra were obtained from samples mounted between NaCl discs. NMR spectra were recorded on a Varian Gemini 2000 instrument (^1H at 300.145 MHz, ^{13}C at 75.479 MHz, ^{31}P at 121.501 MHz). Samples were dissolved in d_6-acetone or C_6D_6 contained in 5 mm sample tubes. Chemical shifts are given in ppm relative to internal tetramethylsilane for ^1H and ^{13}C NMR spectra and external 85% aqueous H_3PO_4 for ^{31}P NMR spectra. UV-vis spectra were recorded on a Varian Cary 5 UV-Vis/NIR spectrometer. Electrospray-ionisation mass spectra (ESI-MS) were obtained with Fisons Platform II (low resolution) or Bruker MicroTOF (high resolution) instruments from samples dissolved in MeOH unless otherwise indicated. Solutions were injected via a 10 ml injection loop. Nitrogen was used as the drying and nebulising gas. Chemical aids to ionisation were used as required [63]. Electrochemical samples (1 mM) were dissolved in CH_2Cl_2 containing 0.5 M [NBu$_4$]BF$_4$ as the supporting electrolyte. Cyclic voltammograms were recorded using a PAR model 263 apparatus, with a saturated calomel electrode and ferrocene as internal calibrant (FeCp$_2$/[FeCp$_2$]$^+$ = +0.46 V vs

33

SCE). A 1 mm path-length cell was used with a Pt-mesh working electrode, Pt wire counter and pseudo-reference electrodes. Elemental analyses were by Campbell Microanalytical Laboratory, University of Otago, Dunedin, New Zealand.

Reagents. The compounds Ru(C≡CC≡CH)(dppe)Cp*,[64] Re(C≡CC≡CH)(CO)$_3$(Bu$^t_2$-bpy) [46] and [M$_2$(μ-dppm)$_2$(MeCN)$_2$]X$_2$ (X = BF$_4$, PF$_6$) [45b, 65-67] were prepared by standard literature methods. In the course of this work, some anomalies in the reported syntheses led us to reinvestigate the nature of some of the binuclear acetonitrile-solvated Cu(I)- and Ag(I)-dppm precursor complexes, which are described elsewhere [67].

4.2.   Ruthenium complexes

(a) [{Cu$_3$(μ-dppm)$_3${μ$_3$-C≡CC≡C[Ru(dppe)Cp]}](BF$_4$)$_2$ [6](BF$_4$)$_2$.* LiBu (0.11 mL of a 2.5 M solution in hexanes, 0.28 mmol) was added rapidly to Ru(C≡CC≡CH)(dppe)Cp* (96 mg, 0.14 mmol) in THF (40 mL) at -20°C. The yellow solution was warmed to r.t., solid [Cu$_2$(μ-dppm)$_2$(NCMe)$_2$](BF$_4$)$_2$ (236.9 mg, 0.21 mmol) was added and the reaction mixture was stirred for 24 h. Evaporation of the resulting orange solution and extraction of the residue with acetone was followed by concentration to ca 2 ml and addition to hexane (50 mL). The orange precipitate was filtered off, washed with hexane and dried in air to give [{Cu$_3$(μ-dppm)$_3${μ$_3$-C≡CC≡C[Ru(dppe)Cp*]}](BF$_4$)$_2$ [6](BF$_4$)$_2$ (188 mg, 61%). The X-ray sample was obtained from acetone. Anal. Calcd (C$_{115}$H$_{105}$B$_2$Cu$_3$F$_8$P$_6$Ru): C, 62.78; H, 4.81. Found: C, 62.82; H, 4.70. IR (Nujol, cm^{-1}): ν(C≡C) 1978. ^{1}H NMR (CDCl$_3$): δ 1.67 (s, 15H, Cp*), 2.30-2.60 (m, 4H, dppe-CH$_2$), 3.09, 3.37 (2 x m, 6H, dppm-CH$_2$), 6.60-7.80 (80H, Ph). ^{13}C NMR (CDCl$_3$): δ 10.9 (s, C$_5$*Me$_5$*), 27.2 (s, dppm-CH$_2$), 30.6 (m, dppe-CH$_2$), 65.6 [C(4)], 94.1, 116.8 [C(2,3)], 95.4 (s, *C$_5$*Me$_5$), 128.0-139.0 (Ph). ^{31}P NMR (CDCl$_3$): δ -8.9 (s, dppm), 78.7 (s, dppe).

(b) [{Cu₃(μ-dppm)₃{μ₃-C≡CC≡C[Ru(dppe)Cp]}](PF₆)₂ [6](PF₆)₂.*

[Cu₂(μ-dppm)₂(NCMe)₄](PF₆)₂ (100 mg, 0.074 mmol) and Ru(C≡CC≡CH)(dppe)Cp* (36 mg, 0.052 mmol) were dried under vacuum before 4:1 THF / NEt₃ (10 mL) was added and the solution heated under reflux for 1 h. The resulting suspension was left to cool to r.t. and the bright orange crystalline product was filtered and washed with diethyl ether to give [{Cu₃(μ-dppm)₃}{μ₃-C≡CC≡C[Ru(dppe)Cp*]}](PF₆)₂ [6](PF₆)₂ (85 mg, 70%). Anal. Calcd (C₁₁₅H₁₀₅Cu₃F₁₂P₁₀Ru): C, 59.63; H, 4.57; M (dication), 2026. Found: C, 59.69; H, 4.63. IR (Nujol, cm⁻¹): ν(C≡C) 1983m; ν(PF) 839s. ¹H NMR (acetone-d_6): δ 1.77 (s, 15H, Cp*), 2.57, 2.89 (2m, 2 x 2H, dppe-CH₂), 3.50 (m, 6H, dppm-CH₂), 7.09-7.89 (80H, Ph). ¹³C NMR (acetone-d_6): 10.9 (s, C₅Me_5), 28.6 (m, CH₂CH₂), 68.1 [septet, $^2J_{CP}$ = 17 Hz, C(4)], 90.6, 117.8 [C(2,3)], 95.7 (s, C_5Me₅), 129.0-137.9 (Ph), 158.4 [t, $^2J_{CP}$ = 21 Hz, C(1)]. ³¹P NMR (acetone-d_6): δ -142.4 (septet, PF₆), -7.8 (s, 6P, dppm), 78.9 (s, 2P, dppe). ESI-MS (m/z): 1013, M²⁺.

(c) [{Ag₃(μ-dppm)₃}{μ₃-C≡CC≡C[Ru(dppe)Cp]}](PF₆)₂ [8](PF₆)₂.* Rapid addition of LiBu (0.08 mL of a 2.5 M solution in hexanes, 0.20 mmol) to a solution of Ru(C≡CC≡CH)(dppe)Cp* (68.4 mg, 0.10 mmol) in THF (40 mL) at -20°C was followed by warming to ambient temperature and addition of [Ag₂(μ-dppm)₂(NCMe)₂](BF₄)₂ (93.2 mg, 0.075 mmol). After stirring over 24 h, solvent was removed from the resulting orange solution. Extraction of the residue with acetone, concentration to ca 2 mL and addition of hexane (50 ml) afforded an orange precipitate, which was recrystallised from acetone to give [{Ag₃(μ-dppm)₃}{μ₃-C≡CC≡C[Ru(dppe)Cp*]}](PF₆)₂ [8](PF₆)₂, identified by ESI-MS (dication at m/z 1080).

(d)   [{Ag₃(μ-dppm)₃}{μ₃-C≡CC≡C[Ru(dppe)Cp]}](BF₄)₂   [8](BF₄)₂.*   Similarly, from Ru(C≡CC≡CH)(dppe)Cp* (96 mg, 0.14 mmol) in THF (40 mL) and LiBu (0.11 mL of a 2.5 M solution in hexanes, 0.228 mmol), followed by solid [Ag₂(μ-dppm)₂(NCMe)₂](BF₄)₂ (261 mg, 0.21 mmol), was obtained orange [Ag₃(μ-dppm)₃}{μ₃-C≡CC≡C[Ru(dppe)Cp*]}](BF₄)₂ [**8**](BF₄)₂ (311 mg, 93%). Pale yellow crystals of the 5THF-solvate suitable for the X-ray study were obtained from THF / hexane. Anal: Calcd (C₁₁₅H₁₀₅Ag₃B₂F₈P₈Ru): C, 59.20; H, 4.54; *M* (dication), 2160. Found: C, 59.21; H, 4.60. IR (nujol, cm⁻¹): ν(C≡C) 1987w, ν(BF) 1051m. ¹H NMR (CDCl₃): δ 1.66 (s, 15H, Cp*), 2.83 (m, 4H, dppe-CH₂), 3.02-4.17 (2m, 6H, dppm-CH₂), 6.70-8.05 (80H, Ph). ³¹P NMR (CDCl₃): δ 2.6 (d, ²J_{PAg} = 365.7 Hz, dppm), 80.5 (s, dppe). ESI-MS (MeOH, *m/z*): (exit-voltage 80 V) 2247.255 ([**8**²⁺ + BF₄⁻]⁺, calcd 2247.238), 1080.130 ([**8**]²⁺, 1080.117), 492.031 ([Ag₂(dppm)₂]²⁺, 492.024); (exit-voltage 150 V) 2247.259 ([**8**²⁺ + BF₄⁻]⁺, 2247.238), 1283.098 ([Ag₂(dppm)Ru(C₄)(dppe)Cp*]⁺, 1283.088), 888.068 ([Ag₃(dppm)₂Ru(C₄)(dppe)Cp*]²⁺, 888.057), 877.152 ([Ag(dppm)₂]⁺, 877.144), 491.028 ([Ag(dppm)]⁺, 491.024).

(e)   [{Cu₃(μ-dppm)₃}{μ₃-C≡CC≡C[Ru(dppe)Cp]}₂]BF₄   [7]BF₄.*   To a solution of Ru(C≡CC≡CH)(dppe)Cp* (57 mg, 0.08 mmol) in 4:1 THF / NEt₃ (10 mL) was added dbu (35 mg, 0.23 mmol) followed by [Cu₂(μ-dppm)₂(MeCN)₄](BF₄)₂ (73 mg, 0.044 mmol). The solution was heated at reflux point for 1 h before cooling and solvent was then removed. The product was extracted into CH₂Cl₂, loaded onto a basic alumina column and eluted with acetone-hexane (2/3). The solvent was then removed and crystallisation of the residue from CH₂Cl₂-hexane gave a bright yellow crystalline solid that was collected and washed with Et₂O to give [{Cu₃(μ-dppm)₃}{μ₃-C≡CC≡C[Ru(dppe)Cp*]}₂]BF₄ [**7**]BF₄ (88 mg, 55%). Anal. Calcd. (C₁₅₅H₁₄₄BCu₃F₄P₁₀Ru₂): C, 66.58; H, 5.19; *M* (cation), 2026. Found: C, 66.85; H, 5.11. IR (Nujol, cm⁻¹): ν(C≡C) 2021w; ν(BF) 1059s. ¹H NMR (C₆D₆): δ 1.56 (s, 30H,

Cp*), 2.56-2.87 (2 x m, 2 x 4H, CH_2CH_2), 3.14-3.17 (m, 6H, dppm), 6.81-7.17 (100H, Ph). ^{13}C NMR (C_6D_6): δ 11.5 (s, C_5Me_5), 28.0-28.2 (m, CH_2CH_2), 64.8 [C(4,5)], 95.0, 117.2 [C(2,3,6,7)], 94.2 (s, C_5Me_5), 121.5 [t, $^2J_{CP}$ = 21 Hz, C(1,8)], 128.0-137.1 (Ph). ^{31}P NMR (C_6D_6): δ -7.3 (s, 6P, dppm), 79.4 (s, 4P, dppe). ESI-MS (MeOH, m/z): 1355, M^{2+}; 635, $[Ru(dppe)Cp^*]^+$.

(f) *[{Cu_3(μ-dppm)_3}{μ_3-C≡CC≡C[Ru(dppe)Cp*]}_2]PF_6* *[7]PF_6*. To a solution of Ru(C≡CC≡CH)(dppe)Cp* (70 mg, 0.10 mmol) in 4:1 THF / NEt_3 (10 mL) was added dbu (45 mg, 0.30 mmol) followed by $[Cu_2(μ\text{-}dppm)_2(NCMe)_4](PF_6)_2$ (100 mg, 0.074 mmol). After the solution was heated at reflux point for 1 h, solvent was removed and the product extracted in CH_2Cl_2 and loaded onto a basic alumina column (20 cm). A yellow band was eluted with acetone-hexane (2/3) and the solvent removed. Crystallisation from CH_2Cl_2-hexane gave a bright yellow crystalline solid that was collected and washed with Et_2O giving [{Cu_3(μ-dppm)_3}{μ_3-C≡CC≡C[Ru(dppe)Cp*]}_2]PF_6 [**7**]PF_6 (102 mg, 70%). Yellow crystals of the acetone solvate for the X-ray study were obtained from acetone / hexane. Anal. Calcd ($C_{155}H_{144}Cu_3F_6P_{11}Ru_2$): C, 65.22; H, 5.08; M (cation), 2026. Found: C, 65.27; H, 4.97. IR (Nujol, cm^{-1}): ν(C≡C) 2018w; ν(PF) 838s. ^1H NMR (acetone-d_6): δ 1.86 (s, 30H, Cp*), 2.58, 3.02 (2m, 2 x 4H, dppe), 3.14 (m, 6H, dppm), 6.76-7.97 (100H, Ph). ^{13}C NMR (acetone-d_6): δ 11.5 (s, C_5Me_5), 28.3 (m, CH_2CH_2), 65.3 [br, C(4,5)], 94.2 (s, C_5Me_5), 94.6, 118.1 [s, C(2,3,6,7)], 121.8 [t, $^2J_{CP}$ = 21 Hz, C(1,8)], 128.4-138.8 (Ph). ^{31}P NMR (acetone-d_6): δ -142.3 (septet, PF_6), -7.5 (s, 6P, dppm), 79.1 (s, 4P, dppe). ESI-MS (m/z): 1355, M^{2+}.

(g) *[{Ag_3(μ-dppm)_3}{μ_3-C≡CC≡C[Ru(dppe)Cp*]}_2]BF_4* *[9]BF_4*. A direct reaction of Ru(C≡CC≡CH)(dppe)Cp* (55 mg, 0.08 mmol) with $[Ag_2(μ\text{-}dppm)_2(MeCN)_2](BF_4)_2$ (75 mg, 0.06 mmol) carried out as for [**7**]BF_4 gave the mustard yellow complex [{Ag_3(μ-dppm)_3}{μ_3-

C≡CC≡C[Ru(dppe)Cp*]}$_2$]BF$_4$ [**9**]BF$_4$ (90 mg, 51%). Anal. Calcd. (C$_{155}$H$_{144}$Ag$_3$BF$_4$P$_{10}$Ru$_2$): C, 63.56; H, 4.96; *M* (cation), 2842. Found: C, 63.77; H, 4.60. IR (Nujol, cm^{-1}): ν(C≡C) 2015 w; ν(BF) 1052s. ^{1}H NMR (C$_6$D$_6$): δ 1.56 (s, 30H, Cp*), 1.79-1.87, 2.53-2.59 (2 x m, 2 x 4H, dppe-CH$_2$), 3.02-3.12 (m, 6H, dppm-CH$_2$), 6.79-7.37 (m, 100H, Ph). ^{13}C NMR (C$_6$D$_6$): δ 10.0 (s, C$_5$*Me$_5$*), 28.85-28.95 (m, CH$_2$), 51.7 [C(4,5)], 95.9, 116.6 [C(2,3,6,7)], 94.2 (s, *C$_5$*Me$_5$), 123.6 [C(1,8)] 128.0-133.8 (Ph). ^{31}P NMR (C$_6$D$_6$): δ -1.2 (s, 6P, dppm), 80.5 (s, 4P, dppe). ESI-MS (acetone, *m/z*): 1421, M^{2+}; 635, [Ru(dppe)Cp*]$^+$.

(h)   [{Ag$_3$(μ-dppm)$_3$}{μ$_3$-C≡CC≡C[Ru(dppe)Cp]}$_2$]PF$_6$ [**9**]PF$_6$.*   To a solution of Ru(C≡CC≡CH)(dppe)Cp* (51 mg, 0.08 mmol) in 4:1 THF / NEt$_3$ (10 mL) was added dbu (35 mg, 0.23 mmol) followed by [Ag$_2$(μ-dppm)$_2$(MeCN)$_2$](PF$_6$)$_2$ (77 mg, 0.06 mmol). The solution was heated at reflux for 1 h in the dark before cooling and solvent was then removed. The residue was dissolved in acetone (5 mL) and added to rapidly stirred Et$_2$O (40 mL). The yellow precipitate was collected and washed with Et$_2$O to give [{Ag$_3$(μ-dppm)$_3$}{μ$_3$-C≡CC≡C[Ru(dppe)Cp*]}$_2$]PF$_6$ [**9**]PF$_6$ (90 mg, 53%). Anal. Calcd. (C$_{155}$H$_{144}$Ag$_3$F$_6$P$_{11}$Ru$_2$): C, 62.32; H, 4.86; *M* (cation), 2842. Found: C, 62.52; H, 5.02. IR (Nujol, cm^{-1}): ν(C≡C) 2033 (w); ν(PF) 838 (s). ^{1}H NMR (C$_6$D$_6$): δ 1.59 (s, 30H, Cp*), 1.77-1.84, 2.51-2.56 (2 x m, 2 x 4H, dppe-CH$_2$), 3.22-3.25 (m, 6H, dppm-CH$_2$), 6.87-7.90 (m, 100H, Ph). ^{13}C NMR (C$_6$D$_6$): δ 9.8 (s, C$_5$*Me$_5$*), 28.2-28.7 (m, CH$_2$), 51.6 [C(4,5)], 94.2 (s, C$_5$*Me$_5$*), 95.8, 116.5 [C(2,3,6,7)], 123.6 [C(1,8)], 127.8-133.6 (Ph). ^{31}P NMR (C$_6$D$_6$): δ -141.1 [sept, $^1J_{PF}$ = 711 Hz, PF$_6$], -1.3 (s, 6P, dppm), 80.7 (s, 4P, dppe). ESI-MS (acetone, *m/z*): 1421, M^{2+}; 635, [Ru(dppe)Cp*]$^+$.

4.3.   Rhenium complexes

The reactions were generally carried out as described earlier,[46c] although the work-up procedure differed.

(a) *[Cu$_3$(dppm)$_3${C≡CC≡C[Re(CO)$_3$(Bu$^t_2$-bpy)}$_2$]PF$_6$* *[10]PF$_6$.* A mixture of Re(C≡CC≡CH)(CO)$_3$(Bu$^t_2$-bpy) (15 mg, 0.025 mmol) and [Cu$_2$(dppm)$_2$(NCMe)$_2$](PF$_6$)$_2$ (25.5 mg, 0.020 mmol) in acetone (5 mL) containing an excess of KOH was stirred at r.t. for 24 h. After removal of solvent, the residue was dissolved in CH$_2$Cl$_2$ / hexane (2/1) and separated on a basic alumina column. The first yellow band eluted with the same solvent mixture contained Re(C≡CC≡CH)(CO)$_3$(Bu$^t_2$-bpy) (2.3 mg, 15%). A red band was eluted with CH$_2$Cl$_2$ / hexane (4/1) and contained [Cu$_3$(dppm)$_3${C≡CC≡C[Re(CO)$_3$(Bu$^t_2$-bpy)}$_2$]PF$_6$ [10]PF$_6$ (21 mg, 61.5%), which was obtained as orange crystals (CH$_2$Cl$_2$ / hexane). IR (CH$_2$Cl$_2$ / cm^{-1}): ν(C≡C) 2136vw, 2074w; ν(CO) 2074s, 1905s(br). ^{1}H NMR (*d$_6$*-acetone): δ 1.49 (s, 36H, 12 Me of Bu^t), 3.01, 3.22 (2 x m, 12 H, 6 dppm), 6.80-7.20 (m, 60H, 12 Ph), 7.92 (d, J_{HH} = 5.9 Hz, 4H, bpy), 8.88 (s, 4H, bpy), 9.27 (d, J_{HH} = 5.9 Hz, 4H, bpy). ^{13}C NMR (*d$_6$*-acetone): δ 27.3-27.8 [m(br), dppm], 30.6 (s, Me), 36.5 (s, *C*-Me), 68.1 (s, C$_\gamma$), 92.1 (s, C$_\beta$), 119.5 (s, C$_\alpha$), 122.2-164.8 (m, Ph + bpy), 192.6, 199.4 (2 x s, CO). ^{31}P NMR (*d$_6$*-acetone): δ -9.1 (s), -12.6 [s(br)] (ratio 2 / 1, dppm), -147.2 (sept, J_{PF} = 707 Hz, PF$_6$).

(b) *[Ag$_3$(dppm)$_3$(Cl){C≡CC≡C[Re(CO)$_3$(Bu$^t_2$-bpy)}]PF$_6$* *[11]PF$_6$.* The solution of Re(C≡CC≡CH)(CO)$_3$(Bu$^t_2$-bpy) (15 mg, 0.025 mmol) and [Ag$_2$(dppm)$_2$(NCMe)$_2$](PF$_6$)$_2$ (22.5 mg, 0.02 mmol) in CH$_2$Cl$_2$ / MeOH (3/1) (7 mL) containing an excess of KOH gradually changed colour from yellow to orange after stirring at r.t. for 24 h. Work-up as in (a) above afforded Re(C≡CC≡CH)(CO)$_3$(Bu$^t_2$-bpy) (1.1 mg, 7%), with an orange band eluted with acetone / hexane (1/2) containing [Ag$_3$(dppm)$_3$(Cl){C≡CC≡C[Re(CO)$_3$(Bu$^t_2$-bpy)}]PF$_6$ [11]PF$_6$ (5.7 mg, 10%), which formed orange crystals (EtOH / Et$_2$O). IR (CH$_2$Cl$_2$ / cm^{-1}): ν(C≡C) 2135vw, 2084w; ν(CO) 2008s, 1908s(br). ^{1}H NMR (*d$_6$*-acetone): δ 1.46 (s, 18H, Me), 2.79, 3.48 (2 x m, dppm), 7.00-7.45 (m, 60H, Ph), 7.87 (d, J_{HH} = 5.9 Hz, 2H of bpy),

8.80 (s, 2H of bpy), 9.16 (d, J_{HH} = 5.9 Hz, 2H of bpy). ^{13}C NMR (d_6-acetone): δ 26.4 (m, dppm), 30.5 (s, Me), 36.5 (s, *C*-Me), 66.1 (s, C_γ), 90.3 (s, C_β) 118.9 (s, C_α), 127.2-164.8 (Ph and bpy), 192.2, 199.1 (2 x s, CO). ^{31}P NMR (d_6-acetone): δ -2.5, -4.3 (2 x m, dppm), -147.3 (sept, J_{PF} = 707 Hz, PF_6). ESI-MS (MeCN / *m/z*): 2099.042, M^+ (calcd 2099.178), 1018.953, $[Ag_2Cl(dppm)_2]^+$ (calcd 1019.018). A light yellow band, eluted with acetone / hexane (1/1), contained known $[Ag_3Cl_2(dppm)_3]PF_6$ (5.5 mg, 29%), identified by ESI-MS and from an X-ray structure. ESI-MS (MeOH / *m/z*): 1546.913, M^+ (calcd 1547.011), 1018.967, $[Ag_2Cl(dppm)_2]^+$ (calcd 1019.018).

(c)   [Ag$_6$(μ-dppm)$_4${C≡CC≡C[Re(CO)$_3$(Bu$^t_2$-bpy)}$_4$](PF$_6$)$_2$ [12](PF$_6$)$_2$. A similar reaction between   Re(C≡CC≡CH)(CO)$_3$(Bu$^t_2$-bpy)   (15   mg,   0.025   mmol)   and $[Ag_2(dppm)_2(NCMe)_2](PF_6)_2$ (25.5 mg, 0.02 mmol) was carried out in THF / NEt$_3$ (4/1) (10 mL) at r.t for 36 h. Work-up as above afforded Re(C≡CC≡CH)(CO)$_3$(Bu$^t_2$-bpy) (2.1 mg, 10.5 %) and yellow-orange $[Ag_6(dppm)_4\{C≡CC≡C[Re(CO)_3(Bu^t_2-bpy)]\}_4](PF_6)_2$ **[12]**(PF$_6$)$_2$ (2.9 mg, 7.2 %), eluted with CH_2Cl_2 / MeOH (20/1) and obtained as orange crystals (CH_2Cl_2 / C_6H_6). This complex was identified by X-ray crystallography.

4.4.   Structure determinations

Full spheres of diffraction data were measured at ca 150 K using CCD area-detector instrumentation [data for **[12]**(PF$_6$)$_2$] were collected at 100 K on the MX1 beamline of the Australia Synchrotron, λ = 0.71073 Å.[68]). All data were measured using monochromatic Mo-*K*α radiation, λ = 0.71073 Å. N_{tot} reflections were merged to *N* unique (R_{int} quoted) after 'empirical'/multiscan absorption correction (proprietary software) and used in the full matrix least squares refinements on F^2, N_o with $F > 4σ(F)$ being considered 'observed'. Anisotropic displacement parameter forms were refined for the non-hydrogen atoms; hydrogen atoms

were treated with a riding model [weights: $(\sigma^2(F_o)^2 + (aP)^2 + (bP))^{-1}$; $P = (F_o^2 + 2F_c^2)/3$]. Neutral atom complex scattering factors were used; computation used the *SHELXL97* or *SHELXL2014* programs [69]. Pertinent results are given above and in Figs. 1 and 2 (which unless otherwise stated show non-hydrogen atoms with 50% probability amplitude displacement ellipsoids and hydrogen atoms having arbitrary radii of 0.1 Å), and in Tables 2-6. CIF data (excluding structure factor amplitudes) have been deposited with the Cambridge Crystallographic Data Centre. CCDC reference numbers: 812795 [**6**]$(BF_4)_2$, 812796 [**8**]$(BF_4)_2$ (acetone solvate), 913187 [**7**]PF_6, 913188 [**8**]$(BF_4)_2$ (THF solvate), 1435455 [**10**]PF_6, 1435410 [**11**]PF_6, 1436607 [**12**]$(PF_6)_2$, 1435449 $[Ag_3(\mu\text{-}dppm)_3Cl_2]PF_6$.

Variata. In the determinations of [**6**]$(BF_4)_2$ and [**8**]$(BF_4)_2$, voids diffusely occupied with solvent residues (acetone) were not susceptible to satisfactory modelling, their contribution being suppressed in the refinements by the use of the program *SQUEEZE* [70]. In the determination of [**8**]$(BF_4)_2 \cdot 5THF$, one disordered THF solvate molecule was refined with isotropic displacement parameters and a total of eight restraints was used to maintain chemically sensible bond lengths and angles for the disordered components.

The structure of [**7**]$PF_6 \cdot 4$acetone has large solvent accessible voids. Seven partially occupied acetone solvate molecules were located in the voids and refined isotropically with occupancies between 0.5 and 0.75. Further residual electron density equating to a unit cell volume of 220 Å^3 contained further peaks which could not be satisfactorily modelled. The thermal ellipsoids for the PF_6 anion are consistent with some disorder of the fluorine atoms on one face of the anion but a chemically sensible disorder model could not be refined. A total of 23 restraints was used in the refinement of the structure; 17 restraints were used to maintain chemically sensible bond lengths and angles for the acetone solvate molecules and F210 (part of the PF_6 anion) was refined using an *ISOR* restraint.

In [**10**]PF$_6$ structure, three CH$_2$Cl$_2$ solvate molecules were identified and refined with 1.0, 0.75 and 0.5 occupancies after trial refinement. Geometries were restrained to ideal values with *SAME* commands and *ISOR* restraints were applied to the C and Cl atoms of the 0.5 occupancy CH$_2$Cl$_2$ solvate molecule. The *SQUEEZE* routine of *PLATON* [70] was applied to the collected data, which resulted in reductions in R_1 and wR_2. R_1, wR_2 and GOF before *SQUEEZE* routine: 7.16%, 22.33% and 1.025; after *SQUEEZE* routine: 6.78%, 18.56%, and 1.067.

For [**11**]PF$_6$, *DFIX* restraints were used to maintain chemically sensible bond lengths for the EtOH solvate molecule in close proximity to the Ag$_3$(dppm)$_3$ entity. The *SQUEEZE* routine of *PLATON* [70] was applied to the collected data, which resulted in reductions in R_1 and wR_2. R_1, wR_2 and GOF before *SQUEEZE* routine: 5.09%, 16.44%, and 1.070; after *SQUEEZE* routine: 4.49%, 12.00%, and 1.105.

Crystals of [Ag$_3$Cl$_2$(dppm)$_3$]PF$_6$ were small and relatively weakly diffracting. There is some disorder / large thermal parameters associated with a single Ph ring of a dppm molecule (C54-C59 and associated H atoms). The Ph ring in question is directed into a cavity formed by the dppm ligands of an adjacent complex. Attempts to model this disorder were unsuccessful.

Crystals of [**12**](PF$_6$)$_2$ were weakly diffracting and required synchrotron radiation to achieve usable diffraction. The Re(CO)$_3$(Bu$^t_2$-bpy) moiety containing Re4 shows some disorder / high thermal displacement and a number of larger residual electron density peaks are located about Re4. The N of a coordinated Bu$^t_2$-bpy ligand and the C of a CO ligand bonded to Re4 were refined with isotropic displacement parameters. *SAME* instructions and *DFIX* restraints were employed in the refinement (40 restraints) to maintain chemically sensible bond lengths and angles for the Re(CO)$_3$(Bu$^t_2$-bpy) moiety containing Re4 and a PF$_6$ anion. A number of C$_6$H$_6$ solvate molecules were located in the difference map and refined

at full or partial occupancy based on trial refinements (solvates with occupancies of 50% or less were refined with isotropic displacement parameters). The structure has large solvent-accessible voids and the *SQUEEZE* routine of *PLATON* [70] was applied to the collected data.

< Tables 5 and 6 here >

Table 5.

Crystal/refinement details for [{M$_3$(μ-dppm)$_3$}{μ$_3$-C≡CC≡C[Ru(dppe)Cp*]}$_2$]X$_2$·nS

Complex	[**6**](BF$_4$)$_2$	[**8**](BF$_4$)$_2$	[**8**](BF$_4$)$_2$	[**7**]PF$_6$
Formula	C$_{115}$H$_{105}$Cu$_3$P$_8$Ru· 2BF$_4$·S	C$_{115}$H$_{105}$Ag$_3$P$_8$Ru· 2BF$_4$·S	C$_{115}$H$_{105}$Ag$_3$P$_8$Ru· 2BF$_4$·5C$_4$H$_8$O	C$_{155}$H$_{136}$Cu$_3$P$_{10}$Ru$_2$· F$_6$P·4C$_3$H$_6$O
MW	2200.1	2333.1	2693.57	3078.4
Crystal system	Orthorhombic	Orthorhombic	Triclinic[*]	Monoclinic[†]
Space group	*Pbca*	*Pbca*	*P*1bar	*P*2$_1$/*n*
a / Å	19.647(3)	20.083(4)	18.5753(9)	15.4381(4)
b / Å	34.033(6)	34.038(8)	18.6769(9)	33.2292(13)
c / Å	37.872(5)	37.711(8)	20.2553(10)	31.2137(9)
V / Å^3	25323(7)	25779(10)	6170.5(5)	15985.1(9)
ρ_c / g.cm^{-3}	1.154	1.202	1.450	1.279
Z (f.u.)	8	8	2	4
μ(Mo-*K*α) / mm^{-1}	0.77	0.71	0.76	0.75
Crystal/mm^3	0.16, 0.15, 0.07	0.18, 0.10, 0.06	0.38, 0.19, 0.04	0.20, 0.15, 0.08
$T_{min/max}$	0.56	0.80	0.82	0.88
2θ$_{max}$ / deg.	50	50	56	57
N_{tot}	246448	167382	93424	143304
N (R_{int})	22316 (0.077)	22897 (0.41)	26131 (0.074)	34429 (0.076)
Reflections *I* > 2σ(*I*)	14124	5550	17265	22179
*R*1 [*I* > 2σ(*I*)]	0.116	0.134	0.058	0.077
*wR*2 (all data)	0.32	0.37	0.152	0.131
S	1.09	0.85	1.04	1.09
|Δρ$_{max}$| e Å^{-3}	1.27	2.21	1.53	1.58

[*] α = 83.513(4), β = 85.582(4), γ = 62.139(5)º. [†] β = 93.349(2)º

44

Table 6. Crystal/refinement details for[M$_3$(μ-dppm)$_3$(X){C≡CC≡C[Re(CO)$_3$ (Bu$^t_2$-bpy)]}]PF$_6$ (M = Cu, X = C≡CC≡C[Re(CO)$_3$(Bu$^t_2$-bpy)]; M = Ag; X = Cl), [Ag$_3$Cl$_2$(dppm)$_3$]PF$_6$ and Ag$_6$(μ-dppm)$_4${C≡CC≡C[Re(CO)$_3$(Bu$^t_2$-bpy)]}$_4$](PF$_6$)$_2$

Compound	[**10**]PF$_6$	[**11**]PF$_6$	[Ag$_3$Cl$_2$(dppm)$_3$]PF$_6$	[**12**](PF$_6$)$_2$
Formula	C$_{125}$H$_{114}$Cu$_3$N$_4$O$_6$P$_6$Re$_2$· PF$_6$· 2¼CH$_2$Cl$_2$	C$_{100}$H$_{84}$Ag$_3$ClN$_2$O$_3$ P$_6$Re PF$_6$· 3EtOH	C$_{75}$H$_{66}$Ag$_3$Cl$_2$P$_6$· PF$_6$	C$_{200}$H$_{184}$Ag$_6$N$_8$O$_{12}$P$_8$ Re$_4$ 2PF$_6$· 5¼C$_6$H$_6$
MW	2853.09	2375.94	1692.57	5231.33
Crystal system	Triclinic[*]	Triclinic[†]	Orthorhombic	Monoclinic[‡]
Space group	$P\bar{1}$bar	$P\bar{1}$bar	$Pbca$	$P2_1/n$
a / Å	15.2538(4)	14.5856(6)	27.611(2)	18.915(4)
b/ Å	17.7777(7)	18.6098(6)	18.2397(7)	33.032(7)
c/ Å	25.8862(9)	21.9744(7)	28.2449(10)	36.635(7)
V / Å^3	6647.3(4)	5412.8(4)	14224.5(13)	22779(8)
ρ_c / g.cm^{-3}	1.425	1.458	1.581	1.525
Z (f.u.)	2	2	8	4
μ(Mo-$K\alpha$) / mm^{-1}	2.521	1.838	1.109	2.757
Crystal/ mm^3	0.35, 0.13, 0.07	0.55, 0.14, 0.06	0.19, 0.08, 0.04	0.25, 0.10, 0.04
$T_{min/max}$	0.70	0.72	0.78	0.75
2θ$_{max}$ / deg.	54	54	54	50
N_{tot}	102724	95301	68081	386380
$N(R_{int})$	28214 (0.062)	26111 (0.052)	17065 (0.172)	53736(0.061)
Reflections $I>2\sigma(I)$	16798	19236	7437	44755
$R_1[I>2\sigma(I)]$	0.0678	0.0455	0.0817	0.1040
wR_2 (all data)	0.186	0.124	0.173	0.2385
S	1.07	1.11	1.00	1.06
$|\Delta\rho_{max}|$ e Å^{-3}	2.256	1.797	1.282	9.080

[*] α = 89.730(3), β = 72.967(3), γ = 82.322(3)º. [†] α = 74.454(3), β = 71.224(4), γ = 79.726(3)º. [‡] β = 95.62(3)º

4.5. Computational details

Density functional calculations were carried out using the Amsterdam density functional (ADF) program [71] developed by Baerends and co-workers [72]. The Vosko-Wilk-Nusair parametrisation [73] was used for the local density approximation (LDA) with gradient correction for exchange (Becke88) [74] and correlation (Perdew86) [75]. The numerical integration procedure applied for the calculations was that developed by teVelde et al. [76]. The atom electronic configurations [77] were described using the basis IV available in the ADF code, i.e., by a triple-ζ Slater-type orbital (STO) basis set for H 1s, C 2s and 2p and P 3s and 3p augmented with a 3d single-ζ polarisation function for C and P and with a 2p single-ζ polarisation function for H. A triple-ζ STO basis set was also used for Cu 3d and 4s, for Ru 4d and 5s, for Ag 4d and 5s, augmented with a single-ζ 4p polarization function for Cu, and with a 5p single-ζ polarization function for Ru and Ag. A frozen-core approximation was used to treat the core shells up to 1s for C, 2p for P, 3p for Cu, 4p for Ru, and 4p for Ag [72]. Geometries were optimized using the analytical gradient method implemented by Verluis and Ziegler [78]. Representation of the molecular orbitals was done using MOLEKEL4.1 [79].

Supplementary Material

Structural representations for [**12**]PF$_6$.

Acknowledgements

References

[1] (a) F. Paul, C. Lapinte, Coord. Chem. Rev. 178-180 (1998) 431;

(b) F. Paul, C. Lapinte, in M. Gielen, R. Willem, B. Wrackmeyer, eds, Unusual Structures and Physical Properties in Organometallic Chemistry, Wiley: New York, (2002).

(c) J.-F. Halet, C. Lapinte, Coord. Chem. Rev. 257 (2013) 1584.

[2] K. Costuas, S. Rigaut, Dalton Trans. 40 (2011) 5643.

[3] (a) P.J. Low, Dalton Trans. (2005) 2821;

(b) P.J. Low, Coord. Chem. Rev. 257 (2013) 1507.

[4] B.S. Brunschwig, N. Sutin, Coord. Chem. Rev 187 (1999) 233.

[5] D.D. Demadis, C.M. Hartshorn, T.J. Meyer, Chem. Rev. 101 (2001) 2655.

[6] M.D. Ward, J.A. McCleverty, Dalton Trans. (2002) 275.

[7] R.L. Roberts, H. Puschmann, J.A.K. Howard, J.H. Yamamoto, A.J. Carty, P.J. Low, Dalton Trans. (2003) 1099.

[8] S.N. Semenov, O. Blacque, T. Fox, K. Venkatesan, H. Berke, J. Am. Chem. Soc. 132 (2010) 3115.

[9] K. Venkatesan, T. Fox, H.W. Schmalle, H. Berke, Organometallics 24 (2005) 2834.

[10] M. Brady, W. Weng, Y. Zhou, J.W. Seyler, A.J. Amoroso, A.M. Arif, M. Bohme, G. Frenking, J.A. Gladysz, J. Am. Chem. Soc. 119 (1997) 775.

[11] V.W.-W. Yam, V.C.Y. Lau, K.K. Cheung, Organometallics, 15 (1996) 1740.

[12] (a) N. Le Narvor, L. Toupet, C. Lapinte, J. Am. Chem. Soc. 117 (1995) 7129;

(b) H.J. Jiao, K. Costuas, J.A. Gladysz, J.-F. Halet, M. Guillemot, L. Toupet, F. Paul, C. Lapinte, J. Am. Chem. Soc. 125 (2003) 9511.

[13] (a) M.I. Bruce, P.J. Low, K. Costuas, J.-F. Halet, S.P. Best, G.A. Heath, J. Am. Chem. Soc. 122 (2000) 1949;

(b) M.I. Bruce, B.G. Ellis, B.W. Skelton, A.H. White, J. Organomet. Chem. 690 (2005) 792.

(c) M. Parthey, J.B.G. Gluyas, P.A. Schauer, D.S. Yufit, J.A.K. Howard, M. Kaupp, P.J. Low, Chem. Eur. J. 19 (2013) 9780.

[14] S. Rigaut, C. Olivier, K. Costuas, S. Choua, O. Fahdel, J. Massue, P. Turek, J.-Y. Saillard, P.H. Dixneuf, D. Touchard, J. Am. Chem. Soc. 128 (2006) 5859.
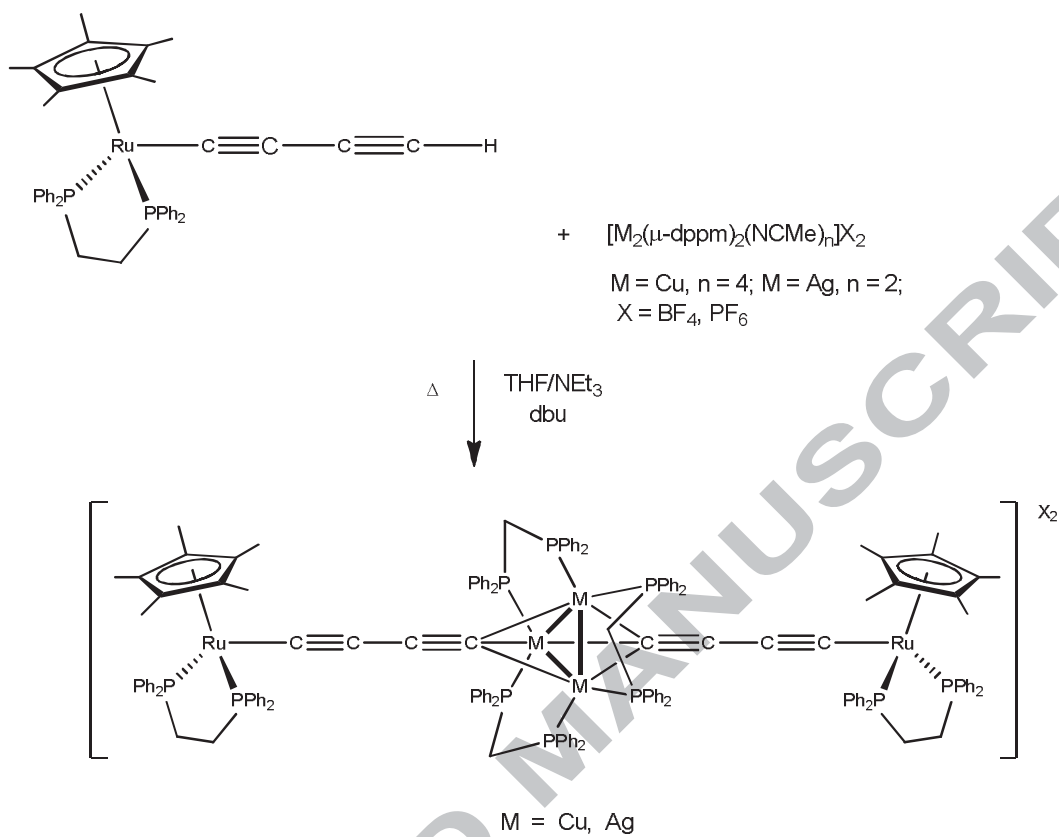
[15] T. Ren, G. Zou, J.C. Alvarez, Chem. Commun. (2000) 1197.

[16] J.L. Bear, B. Han, Z. Wu, E.V. Caemelbecke, K.M. Kadish, Inorg. Chem. 40 (2001) 2275.

[17] M.I. Bruce, K.A. Kramarczuk, B.W. Skelton, A.H. White, J. Organomet. Chem. 695 (2010) 469.

[18] K. Onitsuka, N. Ose, F. Ozawa, S. Takahashi, J. Organomet. Chem. 578 (1999) 169.

[19] W. Mohr, J. Stahl, F. Hampel, J.A. Gladysz, Chem. Eur. J. 9 (2003) 3324.

[20] N.J. Long, C.K. Williams, Angew. Chem. Int. Ed. 42 (2003) 2586.

[21] M.I. Bruce, P.J. Low, Adv. Organomet. Chem. 50 (2004) 179.

[22] M. Parthey, M. Kaupp, Chem. Soc. Rev. 43 (2014) 5067.

[23] V. Balzani, A. Credi, M. Venturi, Molecular Devices and Machines: Concepts and Perspectives for the Nanoworld, 2nd ed., Wiley-VCH: Weinheim, 2008.

[24] K. Costuas, S. Rigaut, Dalton Trans. 40 (2011) 5643.

[25] P. Aguirre-Etcheverry, D. O'Hare, Chem. Rev. 110 (2010) 4839.

[26] S. Záliš, R.F. Winter, W. Kaim, Coord. Chem. Rev. 254 (2010) 1383.

[27] A. Ceccon, S. Santi, L. Orian, A. Busello, Coord. Chem. Rev, 248 (2004) 683.

[28] W. Weng, T. Bartik, M. Brady, B. Bartik, J.A. Ramsden, A.M. Arif, J.A. Gladysz, J. Am. Chem. Soc. 117 (1995) 11922.

[29] Y. Zhu, O. Clot, M.O. Wolf, G.P.A. Yap, J. Am. Chem. Soc. 120 (1998) 1812.

[30] C. Lebreton, D. Touchard, L. Le Pichon, A. Daridor, L. Toupet, P.H. Dixneuf, Inorg. Chim. Acta 272 (1998) 188.

[31] M.I. Bruce, J.-F. Halet, B. Le Guennic, B.W. Skelton, M.E. Smith, A.H. White, Inorg. Chim. Acta 350 (2003) 175.

[32] M. I. Bruce, B. Le Guennic, N. Scoleri, N. N. Zaitseva, J.-F. Halet, Organometallics 31 (2012) 4701.

[33] (a) F. Schwarz, G. Kastlunger, F. Lissel, H. Riel, K. Venkatesan, H. Berke, R. Stadler, E. Lortscher, Nano Lett. 14 (2014) 5932;
(b) F. Lissel, F. Schwarz, O. Blacque, H. Riel, E. Lortscher, K. Venkatesan, H. Berke, J. Am. Chem. Soc. 136 (2014) 14560.

[34] (a) G.-L. Xu, R.J. Crutchley, M.C. DeRosa, Q.-J. Pan, H.-X. Zhang, X. Wang, T. Ren, J. Am. Chem. Soc. 127 (2005) 13354;
(b) B. Xi, G.-L. Xu, P.E. Fanwick, T. Ren, Organometallics 28 (2009) 2338.

[35] (a) J.-W. Ying, I.P.-C. Liu, B. Xi, Y. Song, C. Campana, J.-L. Zuo, T. Ren, Angew. Chem. Int. Ed. 49 (2010) 854.

[36] C.K. Kuo, J.C. Chang, C.Y. Leh, G.H. Lee, C.C. Wang, S.M. Peng, Dalton Trans. (2005) 3696.

[37] J.H.K. Yip, J. Wu, K.Y. Wong, K.P. Ho, C. So-Ngan, J.J. Vittal, Organometallics 21 (2002) 5292.

[38] A. Albinati, F.F. de Biani, P. Leoni, L. Marchetti, M. Pasquali, S. Rizzato, P. Zanello, Angew. Chem. Int. Ed. 44 (2005) 5701.

[39] J.H.K. Yip, J.G. Wu, K.Y. Wong, K.W. Yeung, J.J. Vittal, Organometallics 21 (2002) 1612.

[40] Q.H. Wei, L.Y. Zhang, L.X. Shi, Z.N. Chen, Inorg. Chem. Commun. 7 (2004) 286.

[41] M.I. Bruce, P.J. Low, B.K. Nicholson, B.W. Skelton, N.N. Zaitseva, X.-L. Zhao, J. Organomet. Chem. 695 (2010) 1569.

[42] M.I. Bruce, B.D. Kelly, B.W. Skelton, A.H. White, J. Organomet. Chem. 604 (2000) 150.

[43] (a) R.D. Adams, B. Qu, Organometallics 19 (2000) 4090;
(b) R.D. Adams, B. Qu, M.D. Smith, T.A. Albright, Organometallics 21 (2002) 2970;
(c) R.D. Adams, B. Qu, M.D. Smith, Organometallics 21 (2002) 4847.

[44] A. Arnanz, M.-L. Marcos, S. Delgado, J. González-Velasco, C. Moreno, Dalton Trans. (2009) 168.

[45] (a) M.P. Gamasa, J. Gimeno, E. Lantra, A. Aguirre, S. García-Granda, J. Organomet. Chem. 378 (1989) C11.
(b) J. Diéz, M.P. Gamasa, J. Gimeno, A. Aguirre, S. García-Granda, Organometallics 10 (1991) 380.
(c) J. Diéz, M. P. Gamasa, J. Gimeno, E. Lastra, A. Aguirre, S. García-Granda, Organometallics 12 (1993) 2213.

[46] (a) V.W-W. Yam, K.K-W. Lo, Chem. Soc. Rev. 28 (1999) 323.
(b) V.W-W. Yam, Chem. Commun. (2001) 789.
(c) V.W-W. Yam, W-Y. Lo, C-H. Lam, W.K-M. Fung, K.M-C. Wong, V.C-Y. Lau, N. Zhu, Coord. Chem. Rev. 245 (2003) 39.

[47] (a) V.W-W. Yam, W.K-M. Fung, M-T. Wong, Organometallics 16 (1997) 1772;
(b) V.W-W. Yam, W.K-M. Fung, K-K. Cheung, Organometallics 16 (1997) 2032.
(c) V.W-W. Yam, W.K-M. Fung, K.M-C. Wong, V.C-Y. Lau, K.K. Cheung, Chem. Commun. (1998) 777.
(d) V.W-W. Yam, W.K-M. Fung, K-K. Cheung, Organometallics 17 (1998) 3293.

[48] V.W.-W. Yam, W.-Y. Lo, N. Zhu, Chem. Commun. (2003) 2446.

[49] J.H.K. Yip, J. Wu, K-Y. Wong, K.-W. Yeung, J.J. Vittal, Organometallics 21 (2002) 1612.

[50] M.B. Robin, P. Day, Adv. Inorg. Chem. Radiochem. 10 (1967) 422.

[51] C. Lapinte, J. Organomet. Chem. 693 (2008) 793.

[52] (a) W.E. Geiger, F. Barrière, Acc. Chem. Res. 43 (2010) 1030;

(b) F. Barrière, N. Camire, W.E. Geiger, U.T. Mueller-Westerhoff, R. Sanders, J. Am. Chem. Soc. 124 (2002) 7262.

(c) R. LeSuer, W.E. Geiger, Angew. Chem. Int. Ed. 39 (2000) 248.

[53] D.P. Arnold, G.A. Heath, D.A. James, J. Porphyr. Phthalocyan. 3 (1999) 5.

[54] (a) P. Mucke, R.F. Winter, K. Kowalski, J. Organomet. Chem. 735 (2013) 10.

[55] D.M. D'Alessandro, R.F. Keene, Dalton Trans. (2004) 3950.

[56] P.J. Low, N.J. Brown, J. Cluster Sci. 21 (2010) 235.

[57] R,F. Winter, Organometallics 33 (2014) 4517.

[58] V.W.-W. Yam, W.-Y. Lo, S. C.-F. Lam, K.-K. Cheung, N. Zhu, S. Fathallah, S. Messaoudi, B. Le Guennic, S. Kahlal, J.-F. Halet, J. Am. Chem. Soc. 126 (2004) 7300.

[59] (a) P.K. Mehrotra, R. Hoffmann, Inorg. Chem. 17 (1978) 2187;

(b) K.M. Merz, R. Hoffmann, Inorg. Chem. 27 (1988) 2120.

[60] A. Vega, V. Calvo, E. Spodine, A. Zarate, V. Fuenzalida, J.-Y. Saillard, Inorg. Chem. 41 (2003) 3389.

[61] S. Sculthorpe, P. Braunstein, Chem. Soc. Rev. 40 (2011) 2741.

[62] M.I. Bruce, H.B. Bürgi, J.-F. Halet, B. Le Guennic, B.W. Skelton, A.N. Sobolev, A.H. White, Inorg. Chim. Acta (to be submitted).

[63] W. Henderson, J.S. McIndoe, B.K. Nicholson, P.J. Dyson, J. Chem. Soc., Dalton Trans. (1998), 519.

[64] M.I. Bruce, B.G. Ellis, M. Gaudio, C. Lapinte, G. Melino, F. Paul, B.W. Skelton, M.E. Smith, L. Toupet, A.H. White, Dalton Trans. (2004) 1601.

[65] M.-M. Wu, L.Y. Zhang, Y.-H. Qin, Z.-N. Chen, Acta Crystallogr., Sect. E59 (2003) m195.

[66] M. Lusser, P.Peringer, Polyhedron 4 (1985) 1997.

[67] M.I. Bruce, B.W. Skelton, A.H. White, N.N. Zaitseva, Inorg. Chim. Acta (submitted; Paper ICA-D-16-00692]).

[68] T.M. McPhillips, S.E. McPhlllips, H.J. Chiu, A.E. Cohen, A.M. Deacon, P.J. Ellis, E. Garman, A. Gonzalez, N.K. Sauter, R.P. Phizackerley, S.M. Soltis, P. Kuhn, J. Synchrotron Rad. 9 (2002) 401.

[69] G.M. Sheldrick, Univ. Göttingen, Göttingen, Germany, 2014; ActaCrystallogr. A64 (2008) 112; Acta Crystallogr. C71 (2015) 3.

[70] (a) A.L. Spek, Acta Crystallogr. D65 (2009) 148;

(b) A.L. Spek, ActaCrystallogr. C71 (2015) 9.

[71] Amsterdam Density Functional program (ADF 2000.02 and ADF2010.02); SCM, Theoretical Chemistry, VrijeUniversiteit, Amsterdam, The Netherlands, http://www.scm.com.

[72] (a) C. Fonseca Guerra, J. Snijders, G. te Velde, E.J. Baerends, Theo. Chem. Acc. 99 (1998) 391.

(b) G. te Velde, F.M. Bickelhaupt, C. Fonseca Guerra, S.J.A. van Gisbergen, E.J. Baerends, J. Snijders, T. Ziegler, J. Comput. Chem. 22 (2001) 931.

[73] S.H. Vosko, L. Wilk, M. Nusair, Can. J. Phys. 58 (1980) 1200.

[74] (a) A.D. Becke, J. Chem. Phys. 84 (1986) 4524; (b) A.D. Becke, Phys. Rev. A 38 (1988) 3098.

[75] J.P. Perdew, Phys. Rev. B 33 (1986) 8822.

[76] G. te Velde, E.J. Baerends, J. Comput. Phys. 99 (1992) 84.

[77] E. van Lenthe, E.J. Baerends, J. Comput. Chem. 24 (2003) 1142.

[78] L. Verluis, T. Ziegler, J. Chem. Phys. 88 (1988) 322.

[79] P. Flükiger, H. P. Lüthi, S. Portmann, J. Weber, *MOLEKEL 4.1*, Swiss Center for Scientific Computing, Manno, Switzerland, 2000-2002.

Graphical Absract – Pictogram

$$\text{+} \quad [M_2(\mu\text{-dppm})_2(NCMe)_n]X_2$$

M = Cu, n = 4; M = Ag, n = 2;
X = BF$_4$, PF$_6$

Δ | THF/NEt$_3$
dbu

M = Cu, Ag

Graphical Abstract – Synopsis

Several complexes containing diyndiyl-ML_n [ML_n = Ru(dppe)Cp*, Re(CO)$_3$(Bu$^t_2$-bpy)] fragments bridged by M_3(dppm)3 clusters (M = Cu, Ag) have been obtained from HC$_4$[ML_n] and [M_2(dppm)$_2$(NCMe)$_x$]$^{2+}$ (x = 3,4) and structurally characterised. Electrochemical and DFT studies have shown that the ML_n groups interact with each other through the M_3(dppm)$_3$ cluster.

Highlights

- Complexes containing $M_3(dppm)_3$ clusters (M = Cu, Ag) attached to one or two ML_n fragments [ML_n = Ru(dppe)Cp*, Re(CO)$_3$(Bu$^t_2$-bpy)] have been obtained
- Structural characterisation of several complexes has been achieved
- Electrochemical measurements suggest that the terminal ML_n groups interact through the $M_3(dppm)_3$ cluster
- DFT studies have also been carried out